

Groundwater salinity variation in Upazila Assasuni (southwestern Bangladesh), as steered by surface clay layer thickness, relative elevation and present-day land use

Floris Loys Naus¹, Paul Schot¹, Koos Groen², Kazi Matin Ahmed³, Jasper Griffioen^{1,4}

¹ Copernicus Institute, Environmental Sciences, Utrecht University, Utrecht, The Netherlands

² Acacia water, Gouda, The Netherlands

³ Department of Geology, Dhaka University, Dhaka, Bangladesh

⁴ TNO Geological Survey of the Netherlands, Utrecht, The Netherlands

Correspondence to: Floris Loys Naus (f.l.naus@uu.nl)

Abstract. In the southwestern coastal region of Bangladesh, options for drinking water are limited by groundwater salinity. To protect and improve the drinking water supply, the large variation in groundwater salinity needs to be better understood. This study identifies the palaeo and present-day hydrological processes and their geographical or geological controls that determine variation in groundwater salinity in Upazila Assasuni in southwestern Bangladesh. Our approach involved three steps: a geological reconstruction, based on the literature; fieldwork to collect high density hydrological and lithological data; and data processing to link the collected data to the geological reconstruction in order to infer the evolution of the groundwater salinity in the study area. Groundwater freshening and salinization patterns were deduced using PHREEQC cation exchange simulations and isotope data was used to derive relevant hydrological processes and water sources. We found that the factor steering the relative importance of palaeo and present-day hydrogeological conditions was the thickness of the Holocene surface clay layer. The groundwater in aquifers under thick surface clay layers is controlled by the palaeohydrological conditions prevailing when the aquifers were buried. The groundwater in aquifers under thin surface clay layers is affected by present-day processes, which vary depending on present-day surface elevation. Slightly higher-lying areas are recharged by rain and rainfed ponds and therefore have fresh groundwater at shallow depth. In contrast, the lower-lying areas with a thin surface clay layer have brackish–saline groundwater at shallow depth because of flooding by marine-influenced water, subsequent infiltration and salinization. Recently, aquaculture ponds in areas with a thin surface clay layer have increased the salinity in the underlying shallow aquifers. We hypothesize that to understand and predict shallow groundwater salinity variation in southwestern Bangladesh, the relative elevation and land use can be used as a first estimate in areas with a thin surface clay layer, while knowledge of palaeohydrogeological conditions is needed in areas with a thick surface clay layer.

1 Introduction

In the Ganges–Brahmaputra–Meghna (GBM) river delta, home to 170 million people, availability of safe drinking water is problematic because of the very seasonal rainfall, the likelihood of arsenic occurrence in the shallow groundwater and the pollution of surface water bodies (Harvey et al., 2002; Ravenscroft et al., 2005; Chowdhury, 2010; Sharma et al., 2010; Bhuiyan et al., 2011). In the southwestern coastal region of Bangladesh, suitable drinking water options are even more limited, as here the groundwater is largely brackish to saline

37 (Bahar and Reza, 2010; George, 2013; Fakhruddin & Rahman, 2014; Worland et al., 2015; Ayers et al., 2016).
38 Consequently, the people in this region are at high risk of preeclampsia, eclampsia and gestational hypertension
39 from drinking groundwater, and at increased risk of ingesting pathogens from water from the traditional ponds
40 (Kräzlin, 2000; Khan et al., 2014). Stress on the limited reserves of fresh groundwater is expected to rise in the
41 future through a combination of climate change, sea level rise, increased abstraction for irrigation and industry,
42 and population growth (Shameem et al., 2014; Auerbach et al., 2015). To protect and improve the drinking water
43 supply in the coastal region it is therefore important to understanding the present-day spatial variation and
44 formation processes of the groundwater salinity.

45 Previous studies have found great variation in the groundwater salinity in southwestern Bangladesh
46 (BGS and DHPE, 2001; George, 2013; Worland et al., 2015; Ayers et al., 2016). Several explanations for this
47 large variation have been proposed. One is present-day saline water recharge from the tidal rivers and creeks and
48 the aquaculture ponds that cover much of the region (Rahman et al., 2000; Bahar et al., 2010; Paul et al., 2011;
49 Ayers et al., 2016). Another is freshwater recharge where the clay cover is relatively thin and from rainfed inland
50 water bodies (George, 2013; Worland et al., 2015; Ayers et al., 2016). Finally, some of the variation in the
51 salinity of the groundwater is thought to reflect historical conditions prevailing when the aquifer was buried
52 (George, 2013; Worland et al., 2015; Ayers et al., 2016). Studies in coastal deltas elsewhere, where a higher head
53 due to freshwater infiltration in the higher areas leads to the formation of freshwater lenses, have identified
54 elevation differences as being important factors controlling groundwater salinity (Stuyfzand, 1993; Walraevens
55 et al., 2007; Goes et al., 2009; de Louw et al., 2011; Santos et al. 2012). It has been suggested that both present-
56 day and palaeohydrological processes are important, as deltas are almost never in equilibrium with present-day
57 boundary conditions (Sukhija et al., 1996; Groen et al., 2000; Post and Kooi, 2003; Sivan et al., 2005; Delsman
58 et al., 2014).

59 It remains unclear how each of the proposed processes influences groundwater salinity variation in
60 southwestern Bangladesh. Previous studies found no spatial autocorrelation in groundwater salinity, presumably
61 because the sampling distances were larger than the expected variation in groundwater salinity (Ayers et al.,
62 2016). In our study, we set out to elucidate the hydrological processes that determine the salinity variation in the
63 groundwater by using high density sampling in a case study area with large variation in land use, surface water
64 bodies and surface elevation. In addition, we aimed to identify geographical or geological factors controlling the
65 dominant salinization and freshening processes and, therefore, the groundwater salinity.

66 **2 Methods**

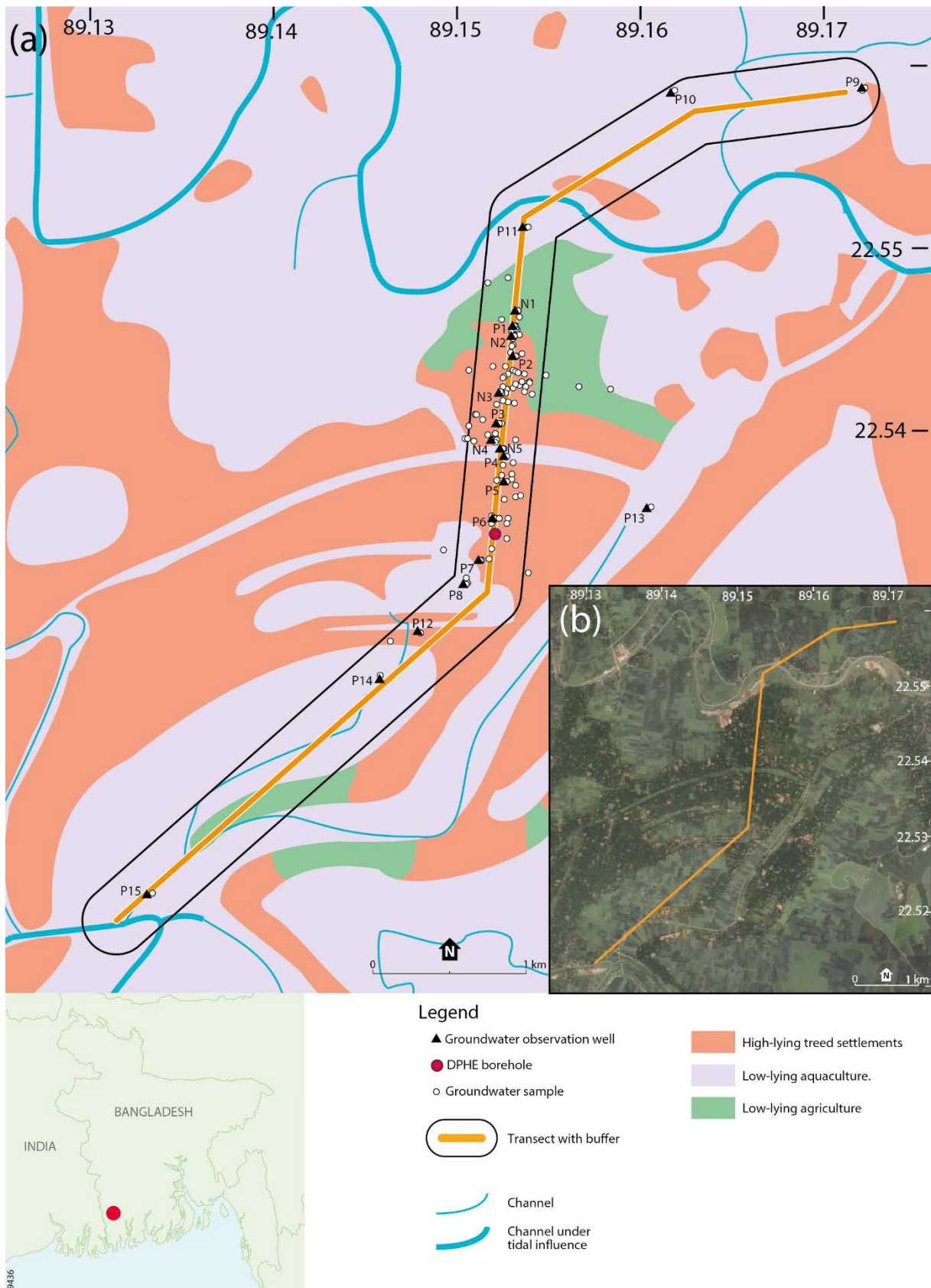
67 **2.1 Methodological approach**

68 Our approach consisted of three steps. First, based on the literature, we reconstructed the geological evolution of
69 southwestern Bangladesh. Second, in the field we carried out high density hydrological and lithological data
70 collection to capture the large expected variation in groundwater salinity. Third, we inferred the evolution of the
71 groundwater salinity by interpreting the field data in the light of the regional geological reconstruction and
72 present-day surface conditions, to determine the dominant processes responsible for the variation in groundwater
73 salinity.

74 **2.2 Fieldwork**

75 To research all the proposed processes, the study area needed to have much variation in land use and surface
76 water bodies, and appreciable variation in surface elevation. We selected an area in southwest Bangladesh by
77 analysing satellite imagery (World Imagery, ESRI, Redlands, CA, USA) to distinguish land use and surface
78 water bodies, Shuttle Radar Topography Mission data (SRTM) (Farr et al., 2007) to analyse elevation patterns
79 and a soil map (FAO, 1959) to ascertain surface geology and geomorphology. The case study area, which is in
80 the Assasuni Upazila (Fig. 1), comprises settlements on slightly higher land, surrounded by lower-lying
81 agricultural fields and aquaculture ponds (Fig. 1). There are freshwater ponds in the settlements. The soil in the
82 study area is composed of fluvial silts in the higher areas and tidal flat clays in the surrounding lower-lying areas
83 (FAO, 1959). The study was conducted along a crooked 6.3 km long transect oriented approximately north–
84 south (Fig. 1) running through several settlements. At the north and south ends are tidal creeks (Fig. 1) whose
85 salinity varies seasonally. They are fresh in the monsoon period, but the salinity slowly rises during the dry
86 season and by April and May the creek water contains up to two thirds seawater (Bhuiyan et al., 2012).

87 In 2017, hydrological and lithological data were collected along the transect at high density (see Sect.
88 2.2.1) to a depth of 50 m in two field campaigns: one in the dry season (January–February) and one in the wet
89 season (July–August). To do so, groundwater observation wells were constructed, the ground was levelled, and
90 surface and groundwater were sampled. The hydrological data were used to establish (1) the present-day
91 variation in groundwater salinity (2) whether groundwater is affected by freshening or salinization (this entailed
92 analysing the cation exchange) and (3) the source water type recharging the groundwater (for this we analysed
93 the isotopic data). The lithological data were linked with the reconstructed geological history to determine the
94 palaeohydrogeological conditions in the study area from the Last Glacial Maximum (LGM) until the present day.



95
96
97
98
99

Figure 1. (a) Overview of the study area, indicating the transect and groundwater observation points, land use and current surface water channels. The land use types are based on satellite imagery (b), SRTM data, a soil map (FAO, 1959) and field observations. The location of the Department of Public Health Engineering (DPHE) borehole is indicated in the figure. (b) Satellite imagery of the study area.

100 **2.2.1 Lithological drillings and groundwater observation wells**

101 Groundwater observation wells were installed to collect lithological information and groundwater samples. In
102 2017, 34 tubes with filters at depths of between 6 and 46 m deep were installed at 20 locations. At 14 locations, a
103 single tube was installed, at four other locations, a nest of two tubes was installed, and at the last four locations, a
104 nest of three tubes was installed. Two groundwater observation wells (P16 and P17) were installed a year later to
105 get more detailed lithological information between P11 and P10, but as the sampling campaign had ended, no
106 water samples are available for them.

107 The first drilling at each location was used to collect the lithological data to approximately 46 m depth
108 (150 feet). The traditional “sludger” or “hand-flapper” method was used as drilling technique (Horneman et al.,
109 2004). The drilling fluid was water from nearby surface water or tube wells, which was pumped out directly after
110 installation by pumping the tube wells for at least 30 minutes or until EC (electrical conductivity) and
111 temperature had stabilized. During the first drilling at each location, the sediment slurry was interpreted in the
112 field every 1.524 m (5 feet). Additional lab analyses were performed on 47 sediment samples from the surface
113 clay layer and at the filter depths. These samples were analysed for their grain size distribution with a Malvern
114 Scirocco 2000, after pre-treatment to remove organic matter and carbonates and after peptizing the mud particles
115 using a peptization fluid and ultrasound. The particles less than 8 μm were classed as clay, those between 8 and
116 63 μm as silt and those over 63 μm as sand (Konert and Vandenberghe, 1997).

117 The carbonate and organic matter contents of the samples were quantified by thermogravimetric
118 analysis (TGA) using a Leco TGA-601. The percentage of organic matter was defined as the weight loss
119 percentage between 150–550°C, corrected for structural water loss from clay by a factor of 0.07 times the
120 fraction smaller than 8 μm (van Gaans et al., 2010; Hoogsteen et al., 2015). The carbonate content was
121 determined as the percentage weight loss between 550 °C and 850 °C.

122 **2.2.2 Elevation**

123 Using a Topcon ES series total station (Topcon, Japan), surface elevation at the installed groundwater
124 observation wells was measured relative to a zero benchmark (a concrete slab at nest 1). The elevation data were
125 used to correlate the wells in terms of their water levels as measured at least two days after installation.

126 **2.2.3 Hydrochemistry and isotopes**

127 During two sampling campaigns, water samples were taken and analysed for anions (IC) and cations (ICP-MS);
128 samples were also taken for tritium analysis, as well as for $\delta^2\text{H}$ and $\delta^{18}\text{O}$ analyses. For details, see Table 1. The
129 groundwater in the groundwater observation wells was sampled at least a week after installation. The household
130 tube wells and groundwater observation wells were purged by pumping approximately three times the volume
131 inside the tube. To sample porewater from the clay, we used the open auger boring method (De Goffau et al.,
132 2012). We drilled a hole with a hand auger, without any drilling fluid. Then we waited for the hole to fill with
133 water, which we sampled by inserting a sample bottle into the hole with a stick, which we pulled back out using
134 a rope that was attached to the bottle. EC, temperature and pH were measured directly in the field using a
135 HANNA HI 9829 (Hanna Instruments, USA). Alkalinity was determined by titration within 36 hours of
136 sampling (Hach Company, USA). The samples were kept out of the sun and cooled as much as possible.

137

138 **Table 1. Overview of chemical and isotope samplings.**

	Samples for IC and ICP-MS (N = 129)	Samples for $\delta^2\text{H}$ and $\delta^{18}\text{O}$ (N = 45)	Samples for tritium (N = 23)
Dry season sampling campaign (January and February 2017)	26 groundwater observation wells, 68 household tube wells, 10 freshwater ponds, 2 aquaculture ponds, 8 open auger borings	-	-
Wet season sampling campaign (July and August 2017)	6 groundwater observation wells, 2 freshwater ponds, 3 aquaculture ponds, 3 open auger borings, 1 inundated field	27 groundwater observation wells, 9 household tube wells, 2 freshwater ponds, 3 aquaculture ponds, 3 open auger boring, 1 inundated field	14 groundwater observation wells, 6 household tube wells, 3 open auger borings

139

140 For the IC and ICP-MS analyses, the water samples were stored in a 15 ml polyethylene tube after filtering
 141 through a 0.45 μm membrane. Back in the Netherlands, aliquots were transferred to 1.5 ml glass vials with
 142 septum caps for IC analysis. For the IC, the aliquots were diluted in accordance with their EC, which was used as
 143 an approximation of their salinity. Below 2000 $\mu\text{S}/\text{cm}$ the aliquots were not diluted (1:0), between 2000 and
 144 4000 $\mu\text{S}/\text{cm}$ the aliquots were diluted two times (1:1), between 4000 and 10000 $\mu\text{S}/\text{cm}$ the aliquots were diluted
 145 five times (1:4), and above 10000 $\mu\text{S}/\text{cm}$ the aliquots were diluted ten times (1:9). The remaining sample was
 146 spiked by adding 100 μl of nitric acid (HNO_3), put on a shaker for 72 hours, and used for ICP-MS. For the ICP-
 147 MS, the chloride concentrations were low enough to allow for direct measurement. However, samples 34, 128,
 148 149, 150, 151, 164, 167, 169, 176, 178 showed matrix effects, so were remeasured after diluting five times. The
 149 samples for isotope analysis ($\delta^2\text{H}$ and $\delta^{18}\text{O}$) were stored in 15 ml polyethylene tubes and analysed on a Thermo
 150 GasBench-II coupled to a Delta-V advantage (Thermo Fisher Scientific, USA). Samples for tritium analysis
 151 were stored in polyethylene 1 litre bottles and analysed according to NEN-EN-ISO 9698.

152 **2.3 Calculations and modelling**

153 **2.3.1 Variations in groundwater salinity**

154 To study salinity variation the water samples were classified on the basis of chloride concentration into four
 155 classes (adjusted from Stuyfzand, 1993): fresh (chloride concentration <150 mg/l) brackish (chloride
 156 concentration 150–1000 mg/l), brackish–saline (chloride concentration 1000–2500 mg/l) and saline (chloride
 157 concentration >2500 mg/l). We estimated the chloride values of observation wells P16 and P17 from their EC
 158 values: we assigned them the chloride values of samples with similar EC values.

159 2.3.2 Interpretation of isotopic composition

160 The stable isotopic composition was interpreted using the mixing line between rainwater and seawater and the
161 Meteoric Water Lines of the two closest meteorological stations with isotopic data: Dhaka and Barisal
162 (respectively 185 km and 125 km from the study area) (IAEA, 2017). For the mixing line between rain and
163 seawater, the weighted average rainwater composition was based on data from the Barisal meteorological station
164 (IAEA, 2017) and the seawater isotopic composition was based on Vienna Standard Mean Ocean Water
165 (VSMOW).

166 2.3.3 Cation exchange

167 Evidence of cation exchange was assessed by calculating the amount of enrichment or depletion of the cations
168 compared to conservative mixing for each sample. Chloride was used as an indicator of the degree of
169 conservative mixing. The deviation from conservative mixing for compound i (in meq/l) was calculated using
170 the following formulae, based on Griffioen (2003):

$$171 \quad iZ = i_{sample} - i_{conservative} \quad (1)$$

172 with:

$$173 \quad i_{conservative} = i_{fresh} + (i_{sea} - i_{fresh}) \cdot \frac{(Cl_{sample} - Cl_{fresh})}{(Cl_{sea} - Cl_{fresh})} \quad (2)$$

174 where i refers to the concentration in meq/l. Seawater is used for the saline end member i_{sea} . To calculate the Z-
175 values we used values from Ganges water (Sarin et al., 1989) and from pond water (this study) for the freshwater
176 end member i_{fresh} . We assumed that Ganges water has had a large influence on the study area for most of the
177 Holocene and that pond water might have influenced the groundwater recently. Z-values had to be negative or
178 positive for both freshwater end members to be accepted as being truly affected by hydrogeochemical processes.
179 To account for false positive or false negative Z-value due to errors in analysis, the Z-values also had to be larger
180 than the expected error for them to be interpreted as affected by hydrogeochemical processes. Like Griffioen
181 (2003), we assumed the expected error in the amount of exchange was 2.8%, based on a standard error in
182 analysis of 2% and standard propagation of error. The same formula was used to indicate whether sulphate had
183 been depleted by reduction or enriched by other sources.

184 2.3.4 PHREEQC simulations of cation exchange

185 For the interpretation of the hydrogeochemical processes that have occurred in each of the groundwater samples,
186 we needed to take account of site-specific conditions and site-specific hydrochemical processes; to do so, we
187 used the PHREEQC model code (Parkhurst and Appelo, 2013). Possible dissolution or precipitation of minerals
188 was assessed by calculating saturation indices for calcite, dolomite and gypsum, and the partial pressure for CO₂.
189 Additionally, cation exchange during salinization or freshening was simulated, to interpret the stage of
190 salinization or freshening for the samples. For salinization, a scenario was simulated in which seawater diluted
191 10 times displaces Ganges water (Sarin et al., 1989). For freshening, two scenarios were simulated, because
192 different cation exchange patterns were expected for a) a scenario in which Ganges water displaces 10 times
193 diluted sea water and b) a scenario in which Ganges water displaces 100 times diluted sea water. The salinities
194 assigned to the saline water end members were based on the salinity levels of mostly less than 1/10th seawater
195 detected in the groundwater.

196 The Z-values of the samples were compared to the Z-values calculated in the PHREEQC scenarios.
197 Freshening or salinization was determined based on the NaZ value of the samples, with a positive NaZ value
198 indicating freshening and a negative NaZ value indicating salinization. Next, the simulated MgZ patterns in the
199 three PHREEQC scenarios were used to differentiate between the stages of freshening or salinization in the
200 groundwater samples.

201 The cation exchange processes were simulated using 1D reactive, advective/dispersive transport. The
202 time steps were 1 year and the groundwater velocity was exactly one cell per time step, which makes the Courant
203 number 1. The dispersivity was taken as half of the velocity, which resulted in a Peclet number of 2. The Courant
204 and Peclet numbers were both within the boundaries of a stable model (Steeffel & MacQuarrie 1996). The Cation
205 Exchange Capacity (CEC) used in the model was based on the value calculated from the empirical variables for
206 marine soils given by Van der Molen (1958):

$$207 \text{CEC} = 6.8 * A + 20.4 * B \quad (3)$$

208 where *A* is the percentage of the particles smaller than 8 µm and *B* is the organic matter percentage, based on
209 values for the 26 sand samples taken in our study. Sulfate reduction and methane production were simulated by
210 introducing CH₂O in a zero-order reaction. For the salinizing scenario, CH₂O was introduced at 0.1 millimoles
211 per year. For the freshening scenario, 0.05 mmol per year were introduced. Based on the calculated saturation
212 indices, calcite dissolution was simulated by keeping the calcite saturation index at 0.25 throughout the run,
213 which is representative for marine water (Griffioen 2017).

214 **3 Results**

215 **3.1 Regional hydrogeological reconstruction**

216 The relevant Holocene sedimentary history of the researched upper 50 m of the subsurface starts in a landscape
217 determined by conditions under the LGM. During the LGM, the sea level was much lower than it is today,
218 leading to fresh conditions. The freshwater rivers eroded deeply incised valleys down to 120 m below the
219 present-day land surface (BGS & DPHE, 2001; Hoque et al., 2014; Mukherjee et al., 2009). In the interfluvial
220 areas, a Pleistocene palaeosol formed, characterized by oxidized sands (Umitsu, 1993; Burgess, 2010; Hoque et
221 al., 2014). The LGM conditions in the study area are uncertain, as the area is near the edge of a possible palaeo-
222 channel (Hoque et al., 2014; Goodbred et al., 2014), making it possible that the starting conditions for the
223 Holocene sedimentation could be either a Pleistocene incised valley or a palaeosol.

224 The Holocene sedimentary history in southwestern Bangladesh can be divided into three distinct
225 periods. First, at around 10–11 kyr BP (kilo years before present), a transgressive period started, when the sea
226 level started to rise rapidly (Islam and Tooley, 1999). In combination with an increase in monsoon intensity
227 (Goodbred and Kuehl, 2000b), this marks the start of a period with very rapid sedimentation (Goodbred and
228 Kuehl, 2000a), leading to a transgressive sediment thickness of 20 to 50 m in nearby study sites (Sarkar et al.,
229 2009; Ayers et al., 2016). The maximum inland location of the shoreline was either slightly south or slightly the
230 north of our study area (Goodbred and Kuehl, 2000a; Shamsudduha and Uddin, 2007). During the transgression,
231 sedimentary conditions are expected to have become more under the influence of marine salinity. In the second
232 period – from 8 kyr BP – sea level rise slowed down, and at ~7 kyr BP the coast started to prograde (Goodbred
233 and Kuehl, 2000a; Sarkar et al., 2009; Goodbred et al., 2014), which probably reduced the influence of marine
234 water. Concomitantly, the monsoon intensity decreased, which caused the sedimentation rate to decline

235 (Goodbred and Kuehl, 2000b; Sarkar et al., 2009). Finally, between 5 kyr and 2.5 kyr BP the Ganges moved
236 eastwards (Allison et al., 2003; Goodbred and Kuehl, 2000a; Goodbred et al., 2003; Goodbred et al., 2014;
237 Morgan and McIntire, 1959; Sarkar et al., 2009). The probable cause of the migration was a topographical
238 gradient resulting from disproportional sedimentation by the Ganges in the west part of the delta (Goodbred et
239 al., 2014), which reduced the supply of sand to the study area, resulting in smaller channels and a larger area of
240 floodplain. In these tidal floodplains, silts and clays were deposited during high water events (Allison et al.,
241 2001), which is why clay overlies all of southwest Bangladesh (BGS and DPHE, 2001; Sarkar et al., 2009; Ayers
242 et al., 2016). Some small late Holocene channels depositing fine sand were still present; sediments from such
243 channels have been found in nearby study areas (Sarkar et al., 2009; Ayers et al., 2016).

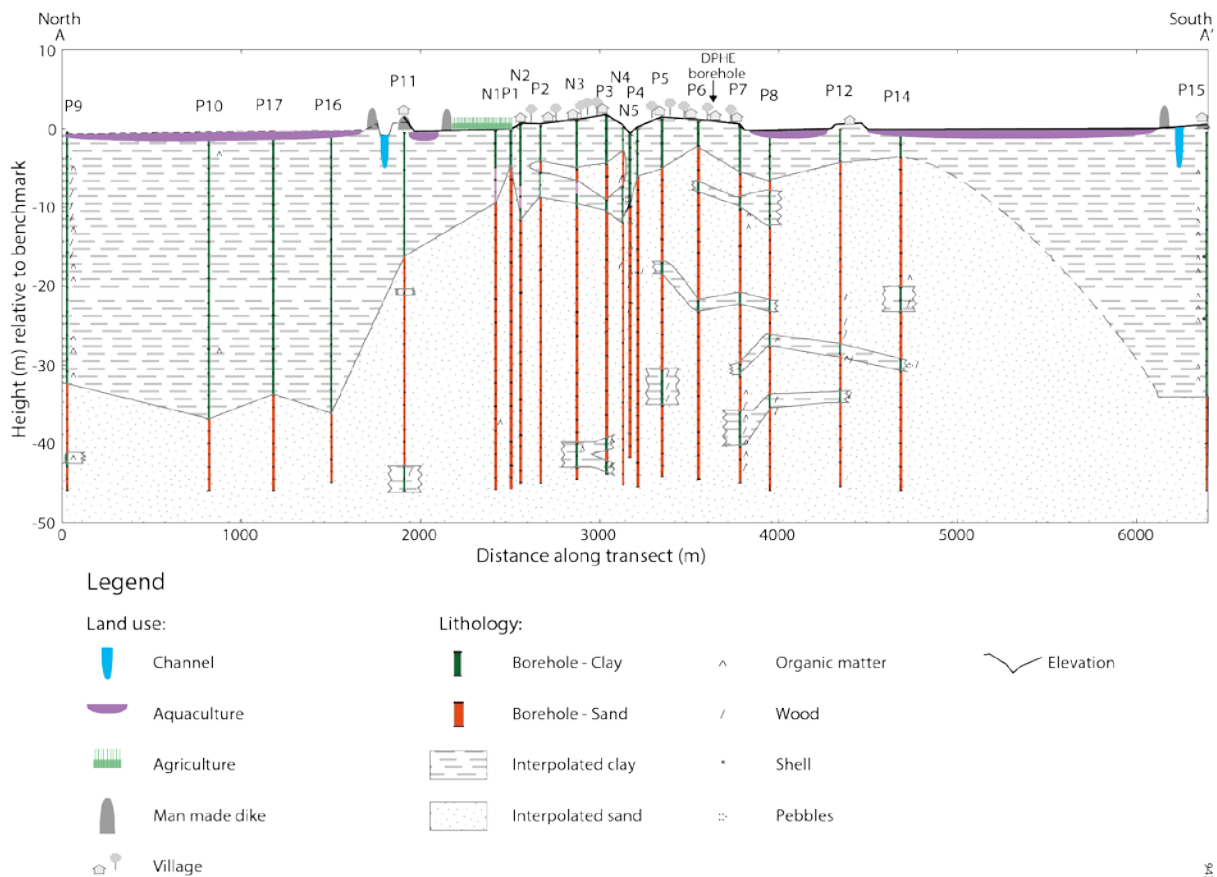
244 Even though the general trend since approximately 7 kyr BP has been progradation, there was a period
245 between 4.5 kyr and 2 kyr BP in which the sea level was higher than it is today (Gupta et al., 1974; Mathur et al.,
246 2004; Sarkar et al., 2009), which might have led to marine deposition at an elevation above present-day sea level
247 (Goodbred et al., 2003; Sarkar et al., 2009).

248 **3.2 Lithology**

249 The collected lithological data reveals a large variation in the thickness and organic matter content of the surface
250 clay layer. In the floodplains in the north at P9, P10, P16 and P17, and in the south at P15, the clay cover is
251 approximately 35 m thick and rich in organic matter (Fig. 2, Table 3), whereas around the settlement in the
252 centre of the transect (henceforth referred to as the central settlement) it is 3–10 m thick and less rich in organic
253 matter (Fig. 2, Table 3). From the middle of the transect towards the north and south, the clay cover becomes
254 gradually thicker (Fig. 2). Under the clay cover is an aquifer composed of grey sands with carbonates, which
255 extends down to the end of all the drillings at 46 m depth (Fig. 2, Table 3). This main aquifer contains some
256 small discontinuous organic-matter-rich clay layers (Fig. 2, Table 3). Extrapolating from a log of the Department
257 of Public Health Engineering (DPHE) for a borehole located between P6 and P7 (Fig. 2), it seems likely that this
258 sand layer extends to 110 m depth and is followed by a clay layer from 110 to 128 m depth and a second aquifer
259 down to a depth of 152 m. At N5, the surface clay layer was succeeded by a gravel bed at 10 m depth.

260 **3.3 Elevation**

261 The villages are at a different elevation than the rest of the study area. Compared with the benchmark, the
262 elevation of the groundwater observation wells in the villages (N2, P2, N3, P3, P5, P6, P7, P11, P12, P15) is
263 between 0.5 to 1.8 m higher, while the elevation in the agricultural fields (N1, P1, N5) and aquaculture ponds
264 (P8, P14) is -0.6 to 0 m (Fig. 2). The elevation was not measured at P9, P10, P16 or P17 but data from the SRTM
265 and field observations suggest that these areas are also relatively low.



266

267 **Figure 2. Lithological data from the boreholes drilled in this study, and the interpolated sand and clay layers. A clear**
 268 **difference in thickness of the clay layer is visible between the palaeo floodplains at the north and south sides of the**
 269 **transect, and the palaeo channel in the middle of the transect.**

270 3.4 Salinity

271 The variation in surface water and groundwater salinity is shown in Fig. 3. Surface and groundwater salinity are
 272 discussed separately below.

273 3.4.1 Surface water salinity

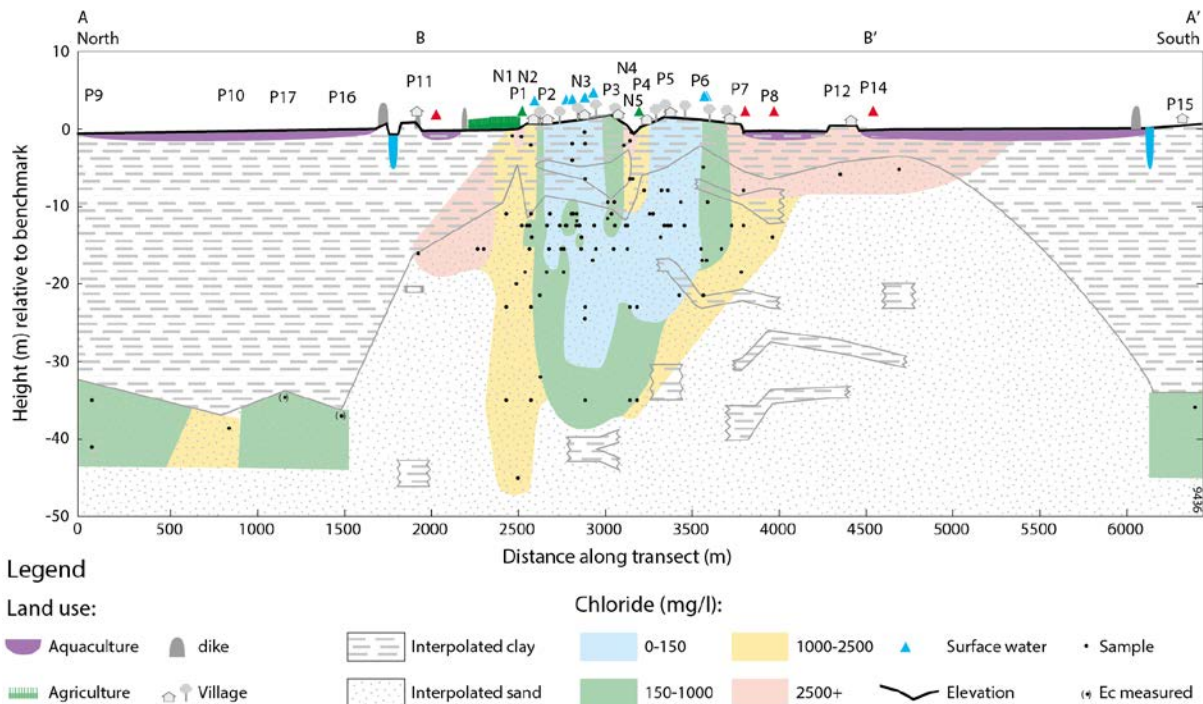
274 The sampled surface water ponds can be divided into fresh and saline ponds. The ponds used for aquaculture
 275 contain slightly less than 25% seawater and have a chloride concentration of around 4000 mg/l, and they are
 276 saline throughout the year. The rainwater ponds in the settlements on higher land have a chloride concentration
 277 below 50 mg/l and are fresh throughout the year. In the wet season, additional surface water bodies are formed,
 278 when many of the agricultural fields become flooded by the large amount of rain. The water in the flooded
 279 agricultural field near N1 and P1 had a chloride concentration around 200 mg/l in July 2017 (Fig. 3), which may
 280 be caused by the dissolution of salts from the saline topsoil, as salt deposits are visible on the surface after the
 281 fields dry out again in the post-monsoon period.

282 3.4.2 Groundwater salinity

283 The chloride concentrations of the groundwater samples vary between 18 mg/l and 4545 mg/l, which indicates
 284 that the most saline groundwater samples contain somewhat less than 25% seawater. The salinity of the
 285 groundwater in the first aquifer correlates well with surface elevation: higher areas are fresher than lower areas

286 (Fig. 3). At the slightly higher central settlements, the groundwater is fresh to a depth of approximately 30 m.
 287 Below that depth, the groundwater is brackish or brackish–saline. In the lower areas with a thick clayey top layer
 288 at the northern and southern ends of the transect, the groundwater is brackish to brackish–saline (Fig. 3). This
 289 was also the case at P16 and P17, where the EC values were respectively 2.49 and 3.4 mS/cm, which – based on
 290 the chloride concentration of samples with similar EC values – corresponds with chloride values between 500
 291 and 1000 mg/l.

292 In low areas with a thin clay cover, groundwater is saline–brackish under the agricultural areas and
 293 saline under the aquaculture ponds. The groundwater salinity difference between these two land use types is
 294 substantial: groundwater chloride concentration under the aquaculture ponds exceeds 4000 mg/l, which is more
 295 than double the groundwater chloride concentration under the agricultural areas (1000–2000 mg/l). The few
 296 samples taken to the side of the transect show the same differences in groundwater salinity between these land
 297 use types. The salinity of water samples taken a few metres below the surface from the clay is generally similar
 298 to that of the groundwater in the sand aquifer immediately below, except for two clay water samples near the
 299 former creek in the middle of the central settlement and one clay water sample from the agricultural fields north
 300 of the central settlement (Fig. 3).



301
 302 **Figure 3. Salinity of the sampled groundwater, of phreatic water sampled in clay just below the surface and of**
 303 **sampled surface water bodies.**

304 **3.5 Stable isotopes**

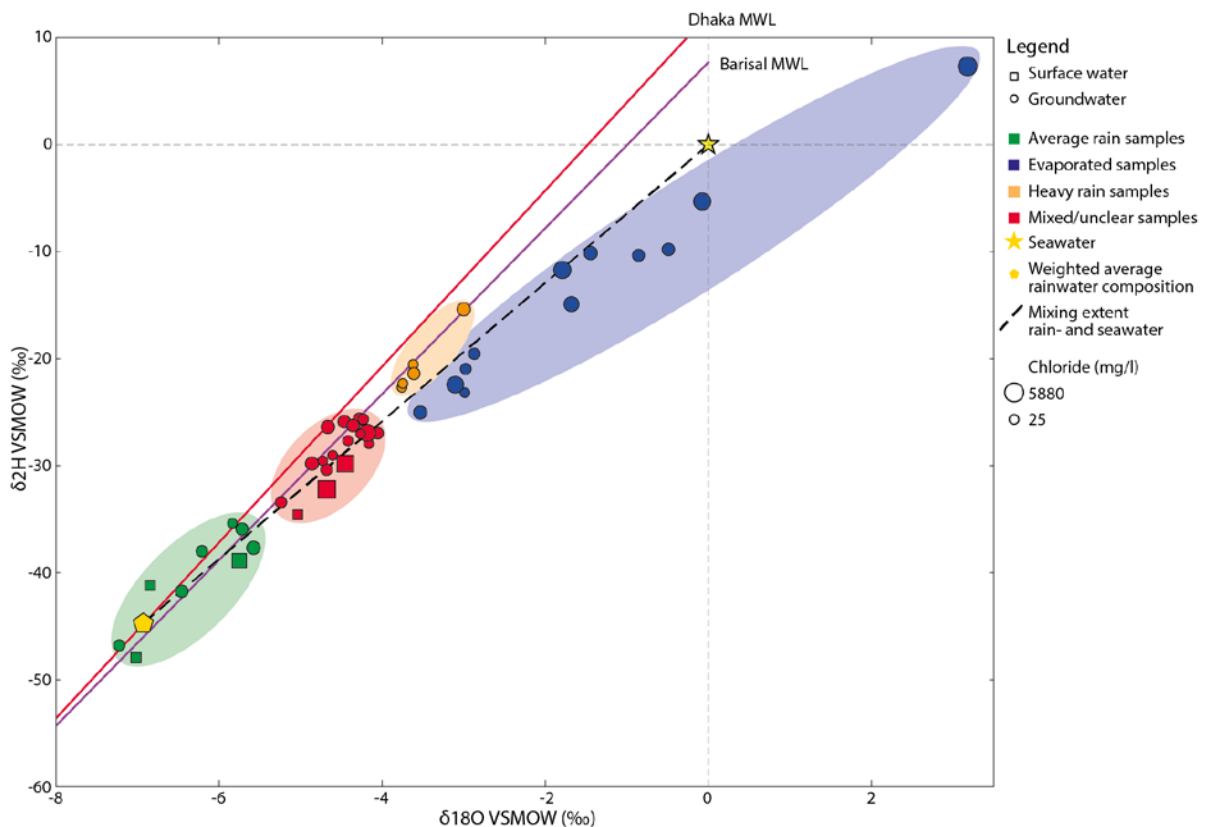
305 The samples were divided into four source water classes (Fig. 4). The first class consisted of samples with a
 306 relatively light isotopic composition, similar to the weighted average rainwater. This indicates that direct rain
 307 infiltration is the dominant source of this water. These samples were taken from surface water bodies in the wet
 308 season. The shallow groundwater sample from the clay layer near N3 also falls in this class, revealing that direct
 309 infiltration of rain occurs to some extent in the higher-lying area. Lastly, the groundwater at P7 and P8, and at
 310 P9, P10 and P15 falls in this class, but since the samples were taken at great depths, or the isotopic composition

311 of overlying groundwater is different, it is unlikely this groundwater formed under present-day conditions (Fig.
312 5).

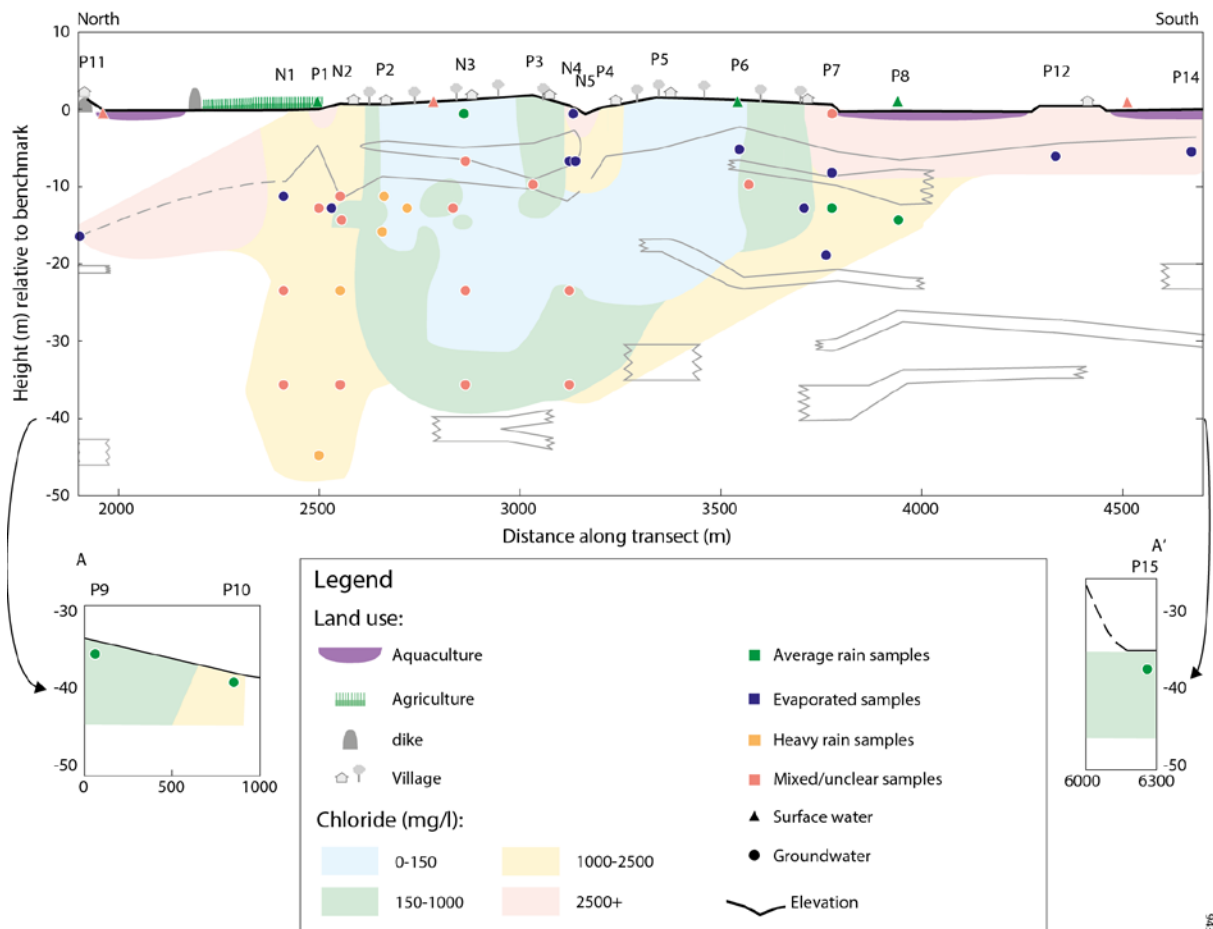
313 The second class contains samples with a relatively heavy isotopic composition skewed to the right of
314 the MWLs (Fig. 4). This indicates an effect of evaporation and mixing with seawater. Samples of this class were
315 taken at relatively shallow depths and close to surface water bodies (Fig. 5), which suggests that the main source
316 of this water is water infiltrating from stagnant surface water.

317 The third class comprises samples with a relatively heavy isotopic composition located close to the
318 MWLs in Fig. 4. In the study area, this class is visible in five groundwater samples taken just north of the central
319 settlements (Fig. 5). The main water source of this class is unclear, but seems to be relatively heavy rain, with
320 limited evaporation or mixing with seawater.

321 The last and largest group is made up of intermediate weight samples without one clear water source
322 type. These samples could be a mix of different sources of water, such as rainwater, water from surface water
323 bodies and seawater. Some influence of surface water bodies is indicated by the small skew to the right from the
324 MWLs. Samples from this class were collected from both fresh and saline water under the thin clay layer (Fig.
325 5).



326
327 **Figure 4. Stable isotope content in the study area. Local Meteoric Water Lines based on monthly samples from the**
328 **two closest stations Dhaka and Barisal at respectively 185 km and 125 km from the study area (IAEA, 2017). The**
329 **mixing line between rainwater and seawater is based on the weighted average rainwater composition from Barisal**
330 **(IAEA, 2017) and seawater VSMOW.**



331
332 **Figure 5. Isotope group of the groundwater sampled in the cross section.**

333 **3.6 Tritium**

334 All 23 samples had a tritium concentration below the detection threshold of 1.64 Bq/l, and therefore tritium
335 content could not be used to date the water. Seawater (<0.4 Bq/l), recent rainwater (0.5 Bq/l), or water older than
336 70 years would all have a tritium concentration below detection threshold, and might therefore be the source of
337 the groundwater (IAEA, 2017).

338 **3.7 Redox conditions and saturation indices**

339 The conditions in the groundwater are reduced, with sulfate reduction and organic matter decay. Sulfate
340 reduction is indicated by depleted sulfate concentrations compared to conservative mixing. Enrichment of SO₄ is
341 observed only in the shallow saline clay near N4 and N5, possibly due to pyrite oxidation. Organic matter decay
342 can be inferred from the partial pressure of CO₂ varying between 10^{-0.4} and 10^{-1.6} atm in most of the groundwater
343 samples, which is high even for tropical conditions, but not unusual in Holocene coastal regions (Appelo and
344 Postma, 2005; Griffioen et al., 2013).

345 Most of the groundwater samples from between 10 and 25 m deep are somewhat supersaturated for
346 calcite, with saturation indices between 0 and 0.7, which is common for seawater-derived groundwater in coastal
347 aquifers (Rezaei et al., 2005; Griffioen et al., 2013). Since the sediments contain carbonates (Appendix; Table 3),
348 calcite, aragonite or dolomite is available for dissolution. The samples that were subsaturated for calcite were
349 taken from the clay cover and the shallow aquifer (<10 m deep).

350 3.8 PHREEQC simulations

351 The Z-values of the groundwater samples were compared with the patterns of the Z-values during the
352 salinization and freshening scenarios (Fig. 6). The patterns of the Z-values were used for the interpretation, as
353 the exact Z-values of the samples were expected to be lower than the Z-values in the model scenarios, since each
354 sample is the result of a specific, less extreme mix of end members. The CaZ, MgZ and NaZ of the groundwater
355 samples were plotted as points in the scenario whose Z-value patterns they best matched, with the X location
356 determined by the chloride concentration matching the values of the chloride in the model scenario. Samples
357 with a chloride concentration exceeding the chloride values in the scenario were plotted at the saline sides of the
358 figures. Six cation exchange (CE) groups were identified (Table 2).

359

360 **Table 2. Cation exchange groups identified.**

Symbol CE group	NaZ value	MgZ value	Description
+	Positive	Positive	Freshening fresh (<200 mg Cl/l)
*	Positive	Negative	Freshening saline (<2000 mg Cl/l)
.	Neutral	Negative, neutral or positive	No cation exchange
-	Negative	Positive	Initial salinization
~	Negative	Neutral	Intermediate salinization
—	Negative	Negative	Late-stage salinization

361

362 3.8.1 Freshening

363 The two freshening scenarios show different patterns for MgZ, because the saline water had a larger percentage
364 of Mg on the cation exchange complex than the fresh water (Appelo et al., 1987; Beekman and Appelo, 1991;
365 Griffioen, 2003). Consequently, the MgZ remained positive during the freshening in the freshwater freshening
366 scenario, while the MgZ became negative during the saline water freshening scenario. We therefore used the
367 MgZ values of the samples to differentiate between freshening freshwater samples (MgZ+) and freshening saline
368 water samples (MgZ-).

369 Freshening freshwater samples came from multiple locations in the shallow (<20 m deep) fresh
370 groundwater in the central settlement, which indicates that this fresh groundwater is likely formed by water
371 infiltrating from the surface. The freshening detected in the deep brackish samples at P9 and P15 is unlikely to
372 be caused by infiltrating fresh surface water, because of the thick impervious clay layer underlying the saline
373 aquaculture water (Fig. 7). Like their isotopic composition, this suggests that this groundwater formed under
374 palaeohydrological conditions.

375 Freshening saline water was detected in three saline samples taken under the agricultural field north of
376 the central village (Fig. 7). The freshening results either from infiltrating surface water, or from fresh water
377 flowing north, as suggested by head data measured in the groundwater observation wells.

378 3.8.2 Salinization

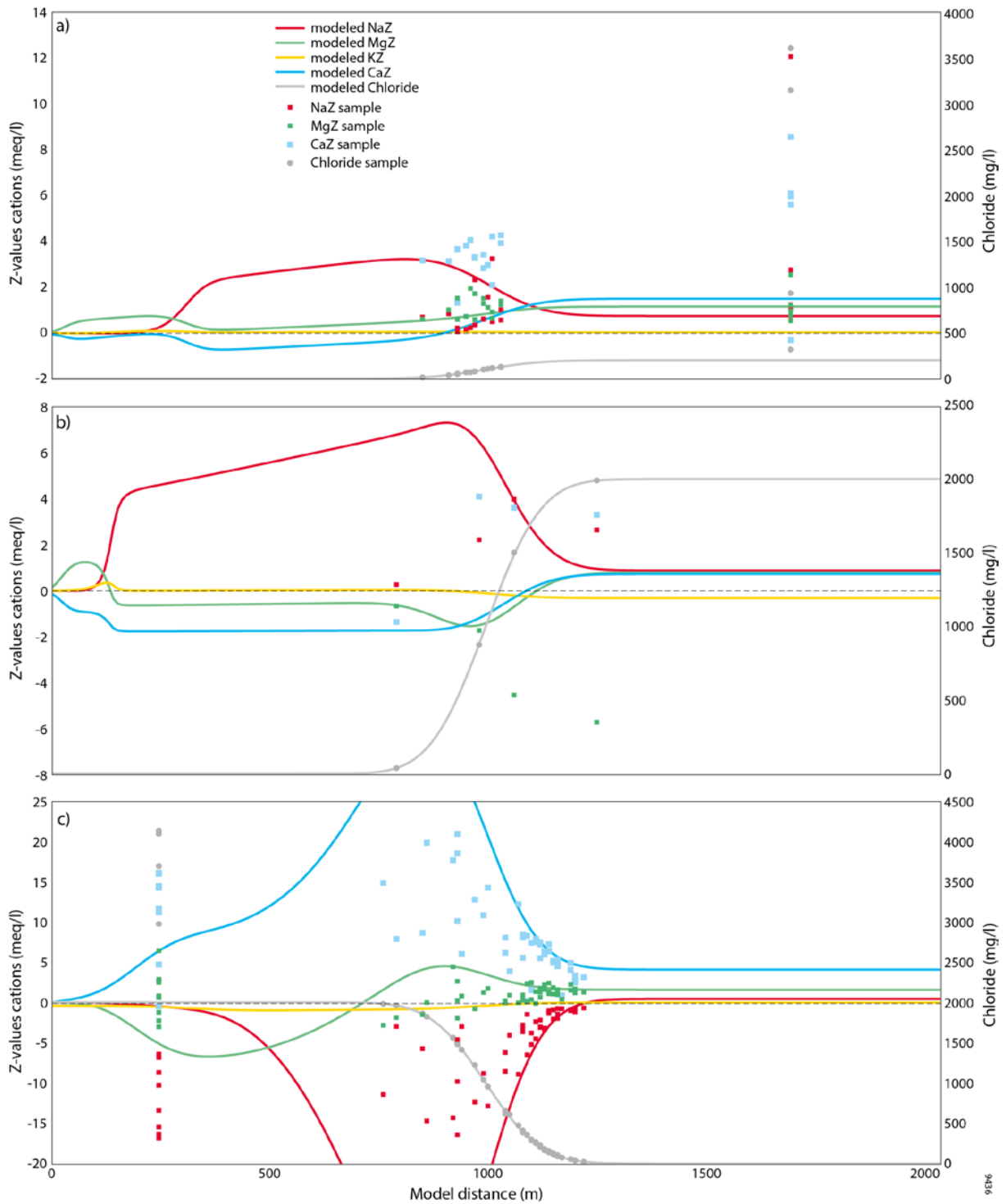
379 In the salinization scenario, the MgZ follows a clear sequence. The MgZ value rises initially, then falls until it
380 becomes negative (Fig. 6). The samples could therefore be divided into three salinization stages: initial
381 salinization with a positive MgZ (- in Fig. 7), intermediate salinization with a neutral MgZ (~ in Fig. 7), and late-
382 stage salinization with a negative MgZ (— in Fig. 7). When initial, intermediate and late-stage salinizing
383 groundwater is found in sequence, the direction of salinization can be interpreted. Groundwater at the
384 salinization front is in the initial stage, behind it is intermediate salinizing groundwater, and finally late-stage
385 salinizing groundwater is close to the source of the saline water.

386 Two clear salinization sequences are observed in the study area. One is south of the central settlement,
387 with late-stage salinization close to the aquaculture ponds followed by intermediate salinization and initial
388 salinization towards the fresh groundwater under the central village (Fig. 7). This sequence indicates that the
389 aquifer has been salinized from the surface of the lower areas. Another salinization sequence is visible at a
390 former creek near N4 and N5 (Fig. 7). Although the clay at the very top is freshening due to recent freshwater
391 recharge, late-stage salinization is visible in the shallow aquifer, followed by intermediate and initial salinization
392 in the brackish and fresh samples at around 12 m depth (Fig. 7). This indicates that some of the groundwater has
393 been salinized by water infiltrating from this former creek.

394 Just north of the central settlement, the salinizing samples lack a clear sequence, but the different
395 salinization stages can still be compared with each other to reveal differences in salinization processes. Under the
396 agricultural fields near N1 and P1 the shallow brackish to fresh-brackish samples display initial salinization,
397 whereas there is late-stage salinization in the samples from depths of 36.5 and 45.7 m. The samples from 36.5 m
398 below the village on higher land again display initial salinization. This suggests that the deeper subsurface under
399 the lower areas has been salinized for longer than the shallower subsurface.

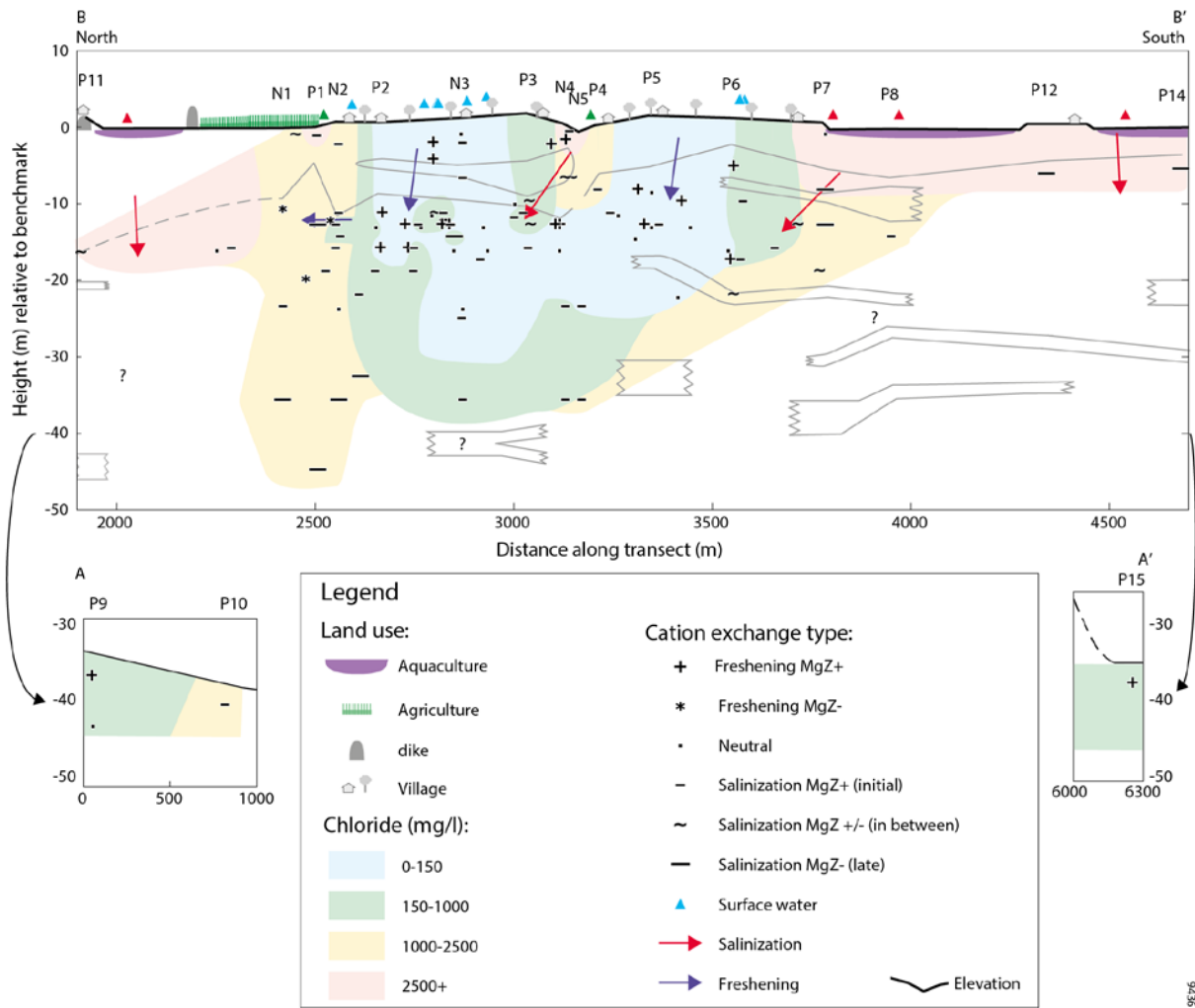
400 The samples taken below the aquaculture ponds at P11, P12 and P14 display intermediate or late-stage
401 salinization, suggesting that they have been salinized by water infiltrating from the aquaculture ponds above.
402 However, as there are no samples close by with different salinization characteristics, it was not possible to
403 determine the direction of this salinization front.

404 Some of the fresh and brackish water samples taken in the central settlement also display salinization.
405 They have probably been salinized by some limited local saline water recharge, as the cation exchange
406 characteristic in the fresh samples is sensitive to small changes in salinity. Near N3, the source of this local
407 salinization is probably water infiltrating from the surrounding low areas, as the salinizing samples were taken
408 close to the edge of the higher-lying area (Fig. 1).



409

410 **Figure 6. Results of the freshwater freshening scenario (A), the saline water freshening scenario (B) and the**
 411 **salinization scenario (C), together with the samples that match each scenario according to the Z-values of their**
 412 **cations. The X location of the samples is determined by the chloride concentration matching the values of the chloride**
 413 **in the scenario. Samples with a chloride concentration exceeding the chloride values in the scenario are plotted at x=**
 414 **250 or x=1750.**



415

416 **Figure 7. Cation exchange types of the sampled groundwater and the phreatic water from the surface clay layer**

417 **4 Discussion**

418 **4.1 Inferred hydrogeological evolution of the study area**

419 Combining the field study results with the geological reconstruction based on literature enabled us to postulate a
 420 reconstruction of the evolution of the lithology and salinity distribution in the groundwater. This evolution is
 421 discussed below, considering the three main Holocene sedimentation phases described earlier plus an additional
 422 phase describing present-day processes.

423 **4.1.1 Phase 1: Filling of an incised valley during Holocene transgression (10ka–7ka BP)**

424 The Pleistocene palaeosol was not observed in the study area, which indicates either that a large incised valley
 425 was present in the Pleistocene, or that a Holocene channel later truncated the palaeosol (Hoque et al. 2014,
 426 Goodbred et al. 2014, Sarkar et al. 2009). This incised valley or truncated Holocene channel filled up rapidly
 427 during the transgression, when a rapid sea level rise combined with an increase in monsoon intensity led to
 428 accelerated sedimentation of channel sands (Fig. 8 (a)) (Islam and Tooley, 1999; Goodbred and Kuehl, 2000a;
 429 Goodbred and Kuehl, 2000b; Sarkar et al., 2009; Ayers et al., 2016). Therefore, the deeper part of the first
 430 aquifer sands must have been during the transgression.

431 **4.1.2 Phase 2: Emergence of large lithological differences (c. 7 kyr– 5/2.5 kyr BP)**

432 At some point in the early Holocene, channel meandering and associated sand deposition became limited to the
433 middle of the transect (Fig. 8 (b)). This is indicated by the switch in sedimentary conditions from sand to clay
434 deposition at approximately 30–35 m depth in the lower-lying areas at P9, P10 in the north, and P15 in the south.
435 The unimodal, poorly sorted grain size distribution of this clay indicates that this switch probably occurred
436 during the progradation (Sarkar et al., 2009). Throughout most of the rest of the Holocene, the areas near P9, P10
437 and P15 remained mangrove-forested tidal delta floodplains, while sand continued to be deposited by the
438 Holocene channel around the present-day central village. The large difference in lithology indicates that the
439 location of the channel was stable throughout the progradation. Possibly, mangrove vegetation in the floodplains
440 prevented the channels from meandering due its ability to capture sediments up to the mean high water level
441 (Furukawa et al., 1996; Auerbach et al., 2015) and to protect land against erosion (Van Santen et al., 2007;
442 Kirwan et al., 2013).

443 This difference in lithology steered the influence of surface water on groundwater during the rest of the
444 Holocene. The groundwater in the sandy aquifer in the middle of the transect continued to be influenced by the
445 fresh surface water conditions, while the aquifers below the floodplains were much more isolated from surface
446 influences by the thick clay layer. The groundwater under the thick clay layer must therefore be controlled by the
447 hydrological conditions at the time of burial. Consequently, the thickness of the clay is the factor controlling the
448 relative importance of palaeohydrological conditions for present-day groundwater salinity. We assume that
449 during the progradation, the salinity at the surface decreased, as evidenced by the freshening cation exchange
450 observed in the brackish groundwater near P9 and P15 (Fig. 3). Additionally, the notion that this groundwater
451 formed under different circumstances than the water close to the present-day central village is reinforced by the
452 different isotopic composition of the groundwater below the thick clay layer compared to the isotopic
453 compositions of the groundwater in the middle of the transect. This process of connate water sealing with
454 subsequent limited influence has also been proposed by George (2013), Worland et al. (2015) and Ayers et al.
455 (2016).

456 **4.1.3 Phase 3: Clay deposition and formation of elevation differences (5/2.5 kyr–present)**

457 **a) Clay deposition**

458 After the Ganges migrated eastwards between 5 kyr and 2.5 kyr BP, the areas that contained large sandy
459 Holocene channels during the progradation also started to develop a clay cover (Fig. 8 (c)) (Goodbred and
460 Kuehl, 2000a; Allison et al., 2003; Goodbred et al., 2003; Sarkar et al., 2009; Goodbred et al., 2014). The
461 salinity during the deposition of the clay cover is not known, as it has been greatly affected by more recent
462 freshening and salinization processes (see phase 4). Overall, however, more brackish conditions are likely to
463 have prevailed from the moment the Ganges migrated eastwards, because the upstream supply of fresh water
464 decreased. Possibly, the deeper groundwater at N1, P1 and N2 has been affected by salinization from this period,
465 since its cation exchange characteristic indicates salinization at a later stage than the shallower samples (Fig. 3).

466 Possibly, starting during the clay deposition in phase 3, salinization of the edges of the aquifer under the
467 thick clay cover has occurred, due to density-driven flow from saline water infiltration in adjacent areas with a
468 thin clay cover (Kooi et al., 2000). In the study area, however, brackish conditions are present at P16 and P17,
469 indicating that density-driven flow has not affected the groundwater immediately below the thick clay layer.

470 This does not mean that density-driven flow is not relevant in the study area. As salinization from density-driven
471 flow mainly consists of vertical convection cells, the resulting salinization can be expected to occur deeper than
472 immediately below the thick clay cover (Kooi et al., 2000; Smith and Turner, 2001).

473 **b) Formation of elevation differences**

474 While the clay cover was being deposited in phase 3, there was probably little difference in elevation. The
475 observed differences in elevation are thought to have come about after the clay deposition, as a result of
476 differences in autocompaction (Allen, 2000; Bird et al., 2004; Tornquist et al., 2008), which can lead to an
477 inversion of surface elevation (Vlam, 1942; van der Sluijs et al., 1965). The thick, organic-matter-rich clays
478 under the floodplains are likely to have been compacted more than the thinner clay cover on the former sand
479 channels, which would account for the present-day elevation differences of up to 1.5 m between the floodplains
480 and the central former channel area in the village on higher land. These elevation differences are similar to those
481 observed in a comparable delta areas in the Netherlands (Vlam, 1942; van der Sluijs et al., 1965).

482 The elevation differences in the middle part of the transect cannot be explained by autocompaction, as
483 here only small changes in lithology are observed. Instead, we hypothesize that they may result from erosion by
484 creeks at the edge of the higher areas. Evidence for this is provided by landforms that look like pathways of
485 erosion caused by meandering tidal creeks north of the central settlement, the tidal creek soils in the areas
486 hypothesized to be affected by erosion, and the distribution of tidal creeks and former tidal creeks in lower-lying
487 areas overlain by thin clay (FAO, 1959). Erosion by tidal creeks implies that the clays originally lay above the
488 average tidal river water level. A possible explanation is clay deposition during the higher sea level between 4.5
489 kyr and 2 kyr BP (Gupta et al. 1974, Mathur et al. 2004, Sarkar et al. 2009). In a subsequent stage, the average
490 water level of the nearby tidal creeks dropped again, resulting in erosive channels.

491 **4.1.4 Phase 4: Emergence of groundwater salinity differences (present-day processes)**

492 **a) Higher areas: Freshening by rain and rainfed ponds**

493 The present-day small differences in elevation result in large differences in groundwater salinity, as the surface
494 elevation has determined whether freshening or salinization has occurred in the groundwater. In the higher-lying
495 areas, the conditions at the surface have mostly been fresh since the elevation differences came about, as the
496 slight elevation has prevented saline water flooding from tides and tidal surges. The fresh groundwater is
497 recharged either by direct infiltration of rainwater, and by infiltration of rainwater stored in man-made ponds.
498 Direct rainwater infiltration, which is a common formation process of freshwater lenses in elevated zones within
499 saline areas (Goes et al., 2009; de Louw et al., 2011; Stuyfzand, 1993; Walraevens et al., 2007), is indicated by
500 the light isotopic composition in the phreatic groundwater from the clay at N3.

501 Infiltration from the rainfed man-made ponds by humans could be a source of fresh groundwater, since
502 they contain fresh water year-round (Harvey et al., 2006; Sengupta et al., 2008). This enables infiltration of fresh
503 water in the dry season when the hydraulic head between the ponds and the groundwater is expected to be larger
504 than in the wet season. The evaporated isotopic composition of the groundwater at P6 suggests such infiltration
505 of pond water (Fig. 5). However, the isotopic composition of the deeper fresh groundwater shows only a small
506 amount of evaporation (Fig. 4, Fig. 5), indicating that infiltration from the freshwater ponds is not the main
507 process responsible for the fresh groundwater – a conclusion reinforced by the usually very low permeability of

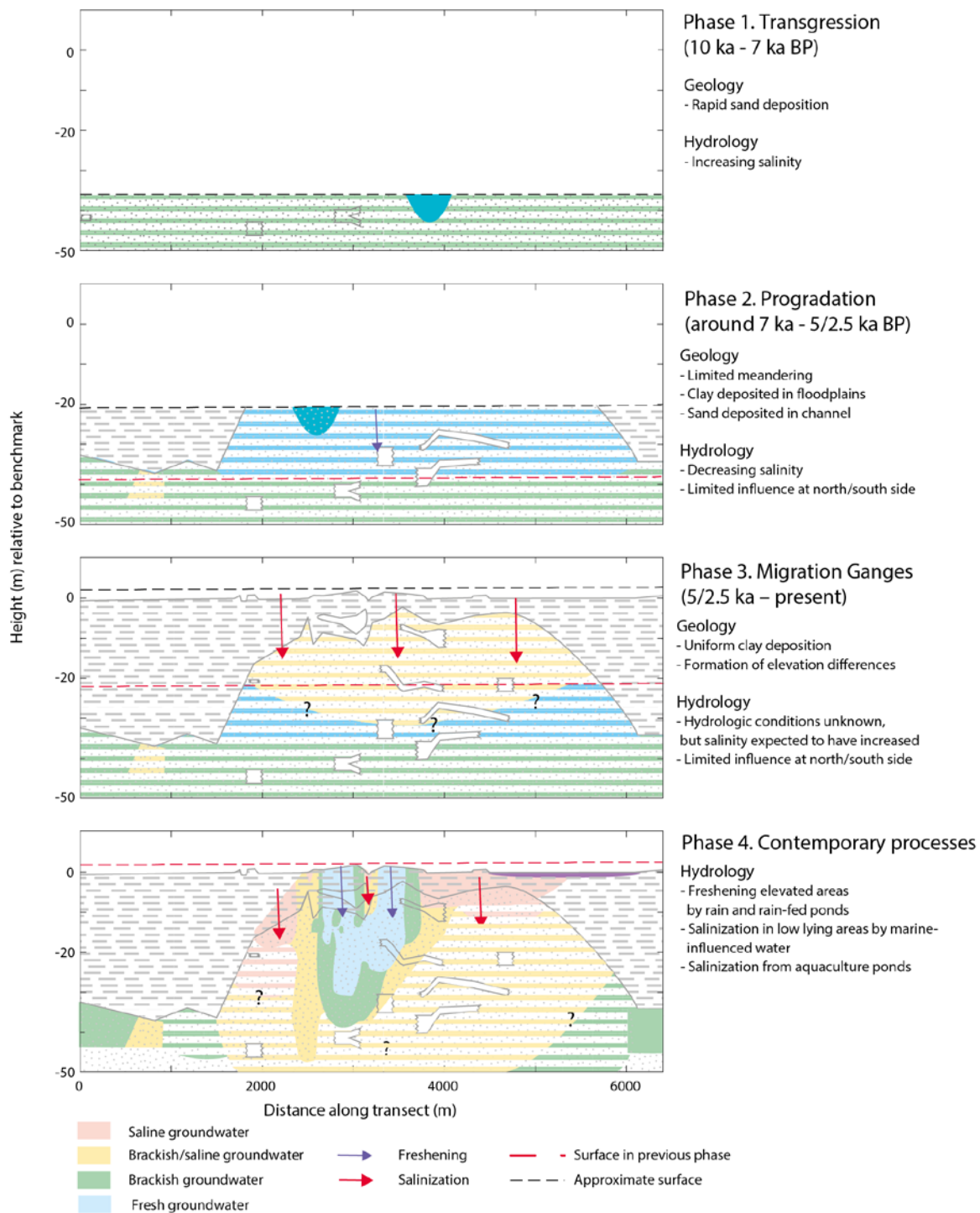
508 the pond bottoms (Sengupta et al., 2008), and the fact that construction of freshwater ponds occurred relatively
509 recently in geological terms (Kräzlin, 2000).

510 **b) Low areas: salinization by marine-influenced water**

511 Unlike the higher areas, the lower areas have often been flooded by tides or tidal surges. Recharge of this saline
512 surface water has been possible in the lower areas with a thin clay cover, where salinizing saline groundwater
513 was observed. This difference between salinization in the lower areas and freshening in the higher areas causes
514 the surface elevation to be the most important factor controlling the salinity of the groundwater in areas with a
515 thin clay cover. Since the salinization originates from the surface, there is already a large difference between
516 higher and lower areas in terms of salinity in the uppermost part of the subsurface, similar to the finding reported
517 by Fernández et al. (2010) for a delta area in Spain. This differs from the situation in Zeeland, the Netherlands,
518 where small fresh groundwater lenses are also present in low-lying areas (Goes et al., 2009; de Louw et al.,
519 2011).

520 Erosion by tidal creeks also occurred in the middle of the central settlement, as visible at the former
521 creek location near N4, N5 and P4, which has salinized the existing fresh groundwater body, as evidenced by the
522 chloride concentrations (Fig. 3) and the sequential salinization patterns (Fig. 7) recharging on top of the fresh
523 groundwater.

524 Recently, aquifers under thin surface clay layers have become salinized by water infiltrating from the
525 overlying aquaculture ponds. This is observed at P11, P7 and P14, where the groundwater has a similar salinity
526 to the overlying aquaculture ponds and an isotopic composition that indicates large evaporation and mixing
527 effects. The salinization by saline aquaculture was detected only in the shallow groundwater underneath saline
528 aquaculture ponds in lower areas with thin surface clay layers. Slightly deeper, the salinization from the shrimp
529 farms was no longer observed; the samples from approximately 12 m deep at P7 and P8 are already much less
530 saline (respectively 1230 and 1370 mg/l), and a totally different isotopic composition (Fig. 3, Fig. 5).
531 Furthermore, no effect was observed in aquifers under thick clay layers. This rather limited influence of saline
532 aquaculture is not unexpected, as saline aquaculture was only introduced in the study area approximately 30
533 years ago (Azad et al., 2009). It does indicate that land use has become a controlling factor for the shallow
534 groundwater salinity in areas with thin surface clay layers. In the future, salinization from aquaculture ponds is
535 expected to continue, and hence the extent of salinization to increase. Since the low-lying aquaculture areas with
536 thin surface clay layers are adjacent to the higher areas, continued salinization from the aquaculture ponds could
537 be a threat for the fresh groundwater under the higher area.



538

539 **Figure 8. Sediment build-up and associated freshening and salinization processes in the study area.**

540 **4.2 Reflection**

541 Above, we derived a hydrogeological evolution of a small area in southwestern Bangladesh, focusing on

542 explaining the large variation in lithology and groundwater salinity which has often been reported in

543 southwestern Bangladesh (BGS and DHPE, 2001; George, 2013; Worland et al., 2015; Ayers et al., 2016).

544 Thanks to the high density of the sampling and the combination of salinity data with isotopic data and

545 PHREEQC-interpreted cation exchange data, it was possible to establish clear patterns in groundwater salinity

546 and to identify relevant hydrological processes and geographical and geological controls. Under the slightly

547 higher area with a thin surface clay layer, a clear pattern of fresh groundwater was identified, which is
548 attributable to recharge by direct infiltration of rain or via rainfed ponds. The presence of such fresh groundwater
549 lenses in this region was postulated by Worland et al. (2015) and Ayers et al. (2016), and the occurrence of fresh
550 groundwater in elevated areas has been described in other brackish or saline deltas (Stuyfzand, 1993;
551 Walraevens et al., 2007; Goes et al., 2009; de Louw et al., 2011; Santos et al. 2012), but to the best of our
552 knowledge, these phenomena in southwestern Bangladesh have never previously been reported in such detail.
553 The fresh groundwater is bordered by brackish and brackish–saline groundwater at greater depth under the
554 higher area and in the direction of the adjacent lower areas, which probably indicates mixing of fresh
555 groundwater with recharged saline flood waters from the lower areas. Saline groundwater is found only at
556 relatively shallow depths below aquaculture ponds in areas with a thin surface clay layer and is attributed to
557 recharge from these present-day aquaculture ponds. Under thick surface clay layers in the lower areas, brackish
558 water is found; it is postulated to be controlled by palaeo salinity conditions at the time of sealing of the sand
559 aquifer. The importance of palaeo conditions for groundwater salinity in isolated parts of the subsurface in this
560 region has been mentioned by others (George, 2013; Worland et al., 2015; Ayers et al., 2016) and has been
561 described in other coastal zones (Sukhija et al., 1996; Groen et al., 2000; Post and Kooi, 2003; Sivan et al.,
562 2005). We postulate the hydrological processes described above and the resulting observed groundwater salinity
563 variation to be primarily steered by three geological and geographical controlling factors: clay cover thickness,
564 relative elevation and present-day land use.

565 We acknowledge our study has several limitations, and our interpretations should be seen as a
566 conceptual model to explain the observed spatial patterns of clay and sand deposits and of groundwater salinity.
567 We did not focus on quantifying recharge, discharge and flow rates, or the exact time scales of the hydrological
568 processes. Without age dating, we can't determine the exact moment of salinization or freshening that has
569 occurred. Additionally, we have been unable to discern comprehensive groundwater flow directions, aside from
570 sketching some indicative flow directions that would account for recharge, as we could not find evidence for
571 locations and patterns of upward groundwater flow and discharge. These upward groundwater flows are
572 expected to be present in convection cells caused by density-driven salinization (Kooi et al., 2000; Smith and
573 Turner, 2001), and discharge is anticipated at drainage points in the landscape which are thought to be present at
574 the edge of higher areas and at the lowest points in the landscape, i.e. the tidal rivers (Tóth, 1963). A possible
575 next step would be to develop a numerical model to further elucidate these flow processes, as well as estimates
576 of recharge and discharge rates and time scales of the described hydrological processes.

577 Despite these limitations, we contend that the identified controlling factors (clay cover thickness,
578 relative elevation and present-day land use) satisfactorily explain an appreciable part of the observed variation in
579 groundwater salinity variation in the larger southwestern Bangladesh region. Relative elevation and land use data
580 could provide a first estimate of the groundwater salinity in areas with a thin surface clay layer, while knowledge
581 of the palaeohydrogeological conditions seems to be necessary to understand and predict the groundwater
582 salinity in areas with a thick surface clay layer. A next step would be to test the validity of this hypothesis at
583 regional scale.

584

585 *Data availability.* The data used in this study is available in the appendix and supplementary material, and may
586 be obtained by contacting the corresponding author.

588 **Table 3. The results of the sediment sample analyses. For the red TGA values no clear peak was identified, indicating**
 589 **influence of TGA noise. For the orange TGA values the peak overlapped the border between the organic matter and**
 590 **the carbonate temperatures.**

Sample number	Sample location	Depth (m)	Grain size percentage						Thermogravimetric analysis	
			% <8 µm	% 8– 63 µm	% 63– 126 µm	% 126– 252 µm	% 252– 502 µm	% >502 µm	% Organic matter (weight loss 150– 550 °C)	% carbonates (weight loss 550– 850 °C)
1	N1	5	15	57	21	5	2	1	1.51	2.43
2	N1	12	2	11	19	52	14	1	0.49	2.02
3	N1	24	0	7	18	51	23	2	0.45	2.01
4	N1	37	16	18	13	30	19	4	1.34	1.90
5	P1	5	40	56	2	0	0	2	0.40	1.13
6	P1	14	1	9	39	44	6	1	0.33	2.58
7	N2	5	14	63	18	4	1	0	1.26	2.79
8	N2	12	5	18	32	40	5	0	0.57	2.33
9	N2	24	1	10	15	48	19	7	0.41	2.04
10	N2	37	0	10	19	46	20	5	0.55	2.15
11	P2	8	6	28	33	24	6	2	0.76	2.69
12	P2	12	0	9	18	54	16	2	0.56	2.15
13	N3	5	41	56	2	0	0	2	0.29	1.84
14	N3	8	2	12	27	48	10	1	0.58	2.02
15	N3	11	15	49	17	14	4	2	2.81	2.57
16	N3	24	1	8	13	44	29	5	0.30	1.87
17	N3	37	0	6	8	32	40	14	0.30	1.96
18	P3	5	30	63	4	1	0	2	0.51	1.63
19	P3	9	0	9	29	44	14	3	0.56	2.23
20	P3	24	0	11	21	35	25	9	1.05	1.97
21	N4	3	22	68	8	1	0	1	0.98	3.23
22	N4	8	1	9	16	40	27	7	4.86	1.56
23	N4	9	11	46	22	14	6	1	1.75	3.37
24	N4	24	0	9	27	48	13	3	0.39	2.50
25	N4	37	0	6	15	50	25	3	0.32	2.14
26	N5	9	15	43	16	17	7	2	1.86	2.99
27	N5	12	0	2	5	30	55	9	0.41	1.33
28	N5	24	0	6	17	58	17	2	0.36	2.18

29	N5	37	0	6	15	44	26	8	0.39	2.14
30	P4	3	24	67	6	1	1	2	1.18	3.63
31	P4	9	0	10	22	48	17	3	0.46	1.70
32	P5	5	22	65	9	2	1	2	1.18	4.26
33	P5	9	2	16	26	38	16	3	0.36	1.82
34	P6	3	14	55	22	6	2	1	0.42	3.73
35	P6	6	0	5	20	49	21	4	0.44	1.97
36	P6	9	7	23	25	36	8	2	1.48	3.00
37	P6	23	0	7	16	52	24	2	0.31	1.82
38	P6	24	17	55	17	6	3	1	3.07	2.63
39	P7	9	2	25	44	20	7	3	0.83	2.89
40	P7	14	1	11	28	39	16	5	1.55	2.07
41	P8	5	12	53	26	7	2	0	1.56	3.07
42	P8	15	0	7	31	43	16	3	0.54	2.15
43	P8	37	1	5	7	33	49	5	4.65	1.50
44	P9	3	32	61	4	0	0	2	1.94	1.73
45	P9	15	26	65	7	1	1	1	3.03	3.53
46	P9	32	23	65	10	1	1	0	4.86	1.65
47	P9	37	1	13	39	39	6	2	0.54	2.92

591

592 *Author contributions.* PPS, KG and KMA wrote the proposal for this study's project. All authors contributed to
593 the focus of the study and the design of the fieldwork campaigns. FLN carried out the fieldwork campaigns,
594 analysed the results and wrote the manuscript with contributions from PPS and JG.

595

596 *Competing interests.* The authors declare that they have no conflict of interest.

597

598 *Acknowledgements.* This work is part of the Delta-MAR project funded by the Urbanizing Deltas of the World
599 programme of NWO-WOTRO. We would like to thank all staff from the Delta-MAR office in Khulna for all
600 their support during the fieldwork, notably Abir Delwaruzzaman for his continued efforts to make sure the
601 fieldwork campaigns were successful. From Dhaka University, Atikul Islam and Pavel Khan are thanked for
602 their field assistance. MSc students Frank van Broekhoven and Rebecca van Weesep (Utrecht University), and
603 Aria Hamann (TU Delft) are acknowledged for helping collect and make a first interpretation of the field data.
604 Dr Joy Burrough is acknowledged for editing a near-final version of the manuscript and Ton Markus is
605 acknowledged for editing the figures.

606 **References**

607 Alam, M.: Geology and Depositional History of Cenozoic Sediments of the Bengal Basin of Bangladesh,
608 Palaeogeogr. Palaeoclimatol. Palaeoecol., 69, 125–139, 1989.

609 Allison, M. A.: Geologic Framework and Environmental Status of the Ganges-Brahmaputra Delta, J. Coast.
610 Res., 14(3), 826–836, doi:10.1017/CBO9781107415324.004, 1998.

- 611 Allison, M. A. and Kepple, E. B.: Modern sediment supply to the lower delta plain of the Ganges-Brahmaputra
612 River in Bangladesh, *Geo-Marine Lett.*, 21(2), 66–74, doi:10.1007/s003670100069, 2001.
- 613 Allison, M. A., Khan, S. R., Goodbred, S. L. and Kuehl, S. A.: Stratigraphic evolution of the late Holocene
614 Ganges–Brahmaputra lower delta plain, *Sediment. Geol.*, 155(3–4), 317–342, doi:10.1016/S0037-
615 0738(02)00185-9, 2003.
- 616 Appelo, C. A. J.: Cation and proton exchange, pH variations, and carbonate reactions in a freshening aquifer,
617 *Water Resour. Res.*, 30(10), 2793–2805, 1994.
- 618 Appelo, C. A. J. and Postma, D.: *Geochemistry, groundwater and pollution*, 2nd ed., A.A. Balkema, Rotterdam.,
619 2004.
- 620 Appelo, C. A. J. and Willemsen, A.: Geochemical calculations and observations on salt water intrusions, I. A
621 combined geochemical/minxing cell model, *J. Hydrol.*, 94(3–4), 313–330, doi:10.1016/0022-1694(87)90058-8,
622 1987.
- 623 Auerbach, L. W., Goodbred Jr, S. L., Mondal, D. R., Wilson, C. a., Ahmed, K. R., Roy, K., Steckler, M. S.,
624 Small, C., Gilligan, J. M. and Ackerly, B. a.: Flood risk of natural and embanked landscapes on the Ganges–
625 Brahmaputra tidal delta plain, *Nat. Clim. Chang.*, 5(2), 153–157, doi:10.1038/nclimate2472, 2015.
- 626 Ayers, J. C., Goodbred, S., George, G., Fry, D., Benneyworth, L., Hornberger, G., Roy, K., Karim, M. R. and
627 Akter, F.: Sources of salinity and arsenic in groundwater in southwest Bangladesh, *Geochem. Trans.*, 17(1), 4,
628 doi:10.1186/s12932-016-0036-6, 2016.
- 629 Bahar, M. M. and Reza, M. S.: Hydrochemical characteristics and quality assessment of shallow groundwater in
630 a coastal area of Southwest Bangladesh, *Environ. Earth Sci.*, 61(5), 1065–1073, doi:10.1007/s12665-009-0427-
631 4, 2010.
- 632 Beekman, H. E., and Appelo, C.A.J.: Ion chromatography of fresh- and salt-water displacement: Laboratory
633 experiments and multicomponent transport modelling, *J. Contam. Hydrol.*, 7(1–2), 21–37, doi:10.1016/0169-
634 7722(91)90036-Z, 1991.
- 635 BGS and DPHE: Arsenic contamination of groundwater in Bangladesh; BGS Technical Report WC/00/19,
636 edited by D. G. Kinniburgh and P. L. Smedley, British Geological Survey, Keyworth., 2001.
- 637 Bhuiyan, M. J. A. N. and Dutta, D.: Assessing impacts of sea level rise on river salinity in the Gorai river
638 network, Bangladesh, *Estuar. Coast. Shelf Sci.*, 96(1), 219–227, doi:10.1016/j.ecss.2011.11.005, 2012.
- 639 Bhuiyan, M. A. H., Rakib, M. A., Dampare, S. B., Ganyaglo, S. and Suzuki, S.: Surface water quality
640 assessment in the central part of Bangladesh using multivariate analysis, *KSCE J. Civ. Eng.*, 15(6), 995–1003,
641 doi:10.1007/s12205-011-1079-y, 2011.
- 642 Burgess, W. G., Hoque, M. A., Michael, H. A., Voss, C. I., Breit, G. N. and Ahmed, K. M.: Vulnerability of
643 deep groundwater in the Bengal Aquifer System to contamination by arsenic, *Nat. Geosci.*, 3(2), 83–87,
644 doi:10.1038/ngeo750, 2010.
- 645 Chowdhury, N. T.: Water management in Bangladesh: an analytical review, *Water Policy*, 12(1), 32,
646 doi:10.2166/wp.2009.112, 2010.
- 647 De Goffau, A., Van Leeuwen, T.C., Van den Ham, A., Doornewaard, G.J., Fraters, B.: Minerals Policy
648 Monitoring Programme Report 2007–2010. Methods and Procedures. National Institute for Public Health and
649 the Environment, Bilthoven, The Netherlands, RIVM Report 680717018, 2012
- 650 de Louw, P. G. B., Eeman, S., Siemon, B., Voortman, B. R., Gunnink, J., van Baaren, E. S. and Oude Essink, G.
651 H. P.: Shallow rainwater lenses in deltaic areas with saline seepage, *Hydrol. Earth Syst. Sci.*, 15(12), 3659–3678,
652 doi:10.5194/hess-15-3659-2011, 2011.
- 653 Esri. "World imagery" [basemap]. Scale Not Given. "World imagery". December 12, 2009.
654 <http://www.arcgis.com/home/item.html?id=10df2279f9684e4a9f6a7f08febac2a9>. (June 11, 2018).
- 655 Fakhruddin, S. H. M. and Rahman, J.: Coping with coastal risk and vulnerabilities in Bangladesh, *Int. J. Disaster
656 Risk Reduct.*, 12, 112–118, doi:10.1016/j.ijdr.2014.12.008, 2014.
- 657 FAO: Soil Survey of the Ganges-Kobadak Area. ETAP Report no. 1071, Rome., 1959.
- 658 Farr, T. G., Rosen, P. A., Caro, E., Crippen, R., Duren, R., Hensley, S., Kobrick, M., Paller, M., Rodriguez, E.,
659 Roth, L., Seal, D., Shaffer, S., Shimada, J., Umland, J., Werner, M., Oskin, M., Burbank, D. and Alsdorf, D.:
660 The Shuttle Radar Topography Mission, *Rev. Geophys.*, 45(2), RG2004, doi:10.1029/2005RG000183, 2007.

- 661 Fernández, S., Santín, C., Marquínez, J. and Álvarez, M. A.: Saltmarsh soil evolution after land reclamation in
662 Atlantic estuaries (Bay of Biscay, North coast of Spain), *Geomorphology*, 114(4), 497–507,
663 doi:10.1016/j.geomorph.2009.08.014, 2010.
- 664 Furukawa, K. and Wolanski, E.: Sedimentation in mangrove forests, *Mangroves Salt Marshes*, 1(1), 3–10,
665 doi:10.1023/A:1025973426404, 1996.
- 666 George, G. J.: Characterization of salinity sources in southwestern Bangladesh evaluated through surface water
667 and groundwater geochemical analyses, Master Thesis, Vanderbilt University., 2013.
- 668 Goodbred, S. L. and Kuehl, S. A.: The significance of large sediment supply, active tectonism, and eustasy on
669 margin sequence development: Late Quaternary stratigraphy and evolution of the Ganges–Brahmaputra delta,
670 *Sediment. Geol.*, 133(3–4), 227–248, doi:10.1016/S0037-0738(00)00041-5, 2000.
- 671 Goodbred, S. L. and Kuehl, S. A.: Enormous Ganges-Brahmaputra sediment discharge during strengthened early
672 Holocene monsoon, *Geology*, 28(12), 1083, doi:10.1130/0091-7613(2000)28<1083:EGSDDS>2.0.CO;2, 2000.
- 673 Goodbred, S. L., Paolo, P. M., Ullah, M. S., Pate, R. D., Khan, S. R., Kuehl, S. A., Singh, S. K. and Rahaman,
674 W.: Piecing together the Ganges-Brahmaputra-Meghna River delta: Use of sediment provenance to reconstruct
675 the history and interaction of multiple fluvial systems during Holocene delta evolution, *Geol. Soc. Am. Bull.*,
676 126(11–12), 1495–1510, doi:10.1130/B30965.1, 2014.
- 677 Goodbred, S. L., Kuehl, S. A., Steckler, M. S. and Sarker, M. H.: Controls on facies distribution and
678 stratigraphic preservation in the Ganges–Brahmaputra delta sequence, *Sediment. Geol.*, 155(3–4), 301–316,
679 doi:10.1016/S0037-0738(02)00184-7, 2003.
- 680 Griffioen, J.: Kation-uitwisselingspatronen bij zoet / zout grondwaterverplaatsingen, *Stromingen*, 9(4), 35–45,
681 2003.
- 682 Griffioen, J.: Enhanced weathering of olivine in seawater: The efficiency as revealed by thermodynamic scenario
683 analysis, *Sci. Total Environ.*, 575, 536–544, doi:10.1016/j.scitotenv.2016.09.008, 2017.
- 684 Griffioen, J., Vermooten, S. and Janssen, G.: Geochemical and palaeohydrological controls on the composition
685 of shallow groundwater in the Netherlands, *Appl. Geochemistry*, 39, 129–149,
686 doi:10.1016/j.apgeochem.2013.10.005, 2013.
- 687 Groen, J., Velstra, J. and Meesters, A. G. C. .: Salinization processes in paleowaters in coastal sediments of
688 Suriname: evidence from $\delta^{37}\text{Cl}$ analysis and diffusion modelling, *J. Hydrol.*, 234(1–2), 1–20,
689 doi:10.1016/S0022-1694(00)00235-3, 2000.
- 690 Gupta, S. K. and Amin, B. S.: Io/U ages of corals from Saurashtra coast, *Mar. Geol.*, 16(5), M79–M83,
691 doi:10.1016/0025-3227(74)90065-6, 1974.
- 692 Harvey, C. F., Swartz, C. H., Badruzzaman, A. B. M., Keon-Blute, N., Yu, W., Ali, M. A., Jay, J., Beckie, R.,
693 Niedan, V., Brabander, D., Oates, P. M., Ashfaque, K. N., Islam, S., Hemond, H. F. and Ahmed, M. F.: Arsenic
694 Mobility and Groundwater Extraction in Bangladesh, *Science.*, 298(5598), 1602–1606,
695 doi:10.1126/science.1076978, 2002.
- 696 Harvey, C. F., Ashfaque, K. N., Yu, W., Badruzzaman, A. B. M., Ali, M. A., Oates, P. M., Michael, H. A.,
697 Neumann, R. B., Beckie, R., Islam, S. and Ahmed, M. F.: Groundwater dynamics and arsenic contamination in
698 Bangladesh, *Chem. Geol.*, 228(1–3), 112–136, doi:10.1016/j.chemgeo.2005.11.025, 2006.
- 699 Hoogsteen, M. J. J., Lantinga, E. A., Bakker, E. J., Groot, J. C. J. and Tittone, P. A.: Estimating soil organic
700 carbon through loss on ignition: effects of ignition conditions and structural water loss, *Eur. J. Soil Sci.*, 66(2),
701 320–328, doi:10.1111/ejss.12224, 2015.
- 702 Hoque, M. A., McArthur, J. M. and Sikdar, P. K.: Sources of low-arsenic groundwater in the Bengal Basin:
703 investigating the influence of the last glacial maximum palaeosol using a 115-km traverse across Bangladesh,
704 *Hydrogeol. J.*, 22(7), 1535–1547, doi:10.1007/s10040-014-1139-8, 2014.
- 705 IAEA/WMO: Global Network of Isotopes in Precipitation. The GNIP Database, [online] Available from:
706 <http://www.iaea.org/water> (Accessed 26 September 2017), 2017.
- 707 Islam, M. S. and Tooley, M. J.: Coastal and sea-level changes during the Holocene in Bangladesh, *Quat. Int.*,
708 55(1), 61–75, doi:10.1016/S1040-6182(98)00025-1, 1999.
- 709 Kakiuchi, H., Momoshima, N., Okai, T. and Maeda, Y.: Tritium concentration in ocean, *J. Radioanal. Nucl.*
710 *Chem.*, 239(3), 523–526, doi:10.1007/BF02349062, 1999.

711 Khan, A. E., Scheelbeek, P. F. D., Shilpi, A. B., Chan, Q., Mojumder, S. K., Rahman, A., Haines, A. and Vineis,
712 P.: Salinity in Drinking Water and the Risk of (Pre)Eclampsia and Gestational Hypertension in Coastal
713 Bangladesh: A Case-Control Study, edited by P. B. Szecsi, *PLoS One*, 9(9), e108715,
714 doi:10.1371/journal.pone.0108715, 2014.

715 Kirwan, M. L. and Megonigal, J. P.: Tidal wetland stability in the face of human impacts and sea-level rise,
716 *Nature*, 504(7478), 53–60, doi:10.1038/nature12856, 2013.

717 Konert, M. and Vandenberghe, J.: Comparison of laser grain size analysis with pipette and sieve analysis: a
718 solution for the underestimation of the clay fraction, *Sedimentology*, 44(3), 523–535, doi:10.1046/j.1365-
719 3091.1997.d01-38.x, 1997.

720 Kooi, H., Groen, J. and Leijnse, A.: Modes of seawater intrusion during transgressions, *Water Resour. Res.*,
721 36(12), 3581–3589, doi:10.1029/2000WR900243, 2000.

722 Kränzlin, I.: Pond management in rural Bangladesh: problems and possibilities in the context of the water supply
723 crisis, *Nat. Resour. Forum*, 24(3), 211–223, doi:10.1111/j.1477-8947.2000.tb00945.x, 2000.

724 Mathur, U. B., Pandey, D. K. and Bahadur, T.: Falling Late Holocene sea-level along the Indian coast, *Curr. Sci.*,
725 87(4), 439–440, 2004.

726 McGranahan, G., Balk, D. and Anderson, B.: The rising tide: assessing the risks of climate change and human
727 settlements in low elevation coastal zones, *Environ. Urban.*, 19(1), 17–37, doi:10.1177/0956247807076960,
728 2007.

729 Mondal, M. K., Bhuiyan, S. I. and Franco, D. T.: Soil salinity reduction and prediction of salt dynamics in the
730 coastal ricelands of Bangladesh, *Agric. Water Manag.*, 47(1), 9–23, doi:10.1016/S0378-3774(00)00098-6, 2001.

731 Morgan, J. P. and McIntire, W. G.: Quarternary Geology of the Bengal Basin, East Pakistan and India, *Geol.*
732 *Soc. Am. Bull.*, 70(3), 319–342, doi:10.1130/0016-7606(1959)70[319:QGOTBB]2.0.CO;2, 1959.

733 Mukherjee, A., Fryar, A. E. and Thomas, W. A.: Geologic, geomorphic and hydrologic framework and evolution
734 of the Bengal basin, India and Bangladesh, *J. Asian Earth Sci.*, 34(3), 227–244,
735 doi:10.1016/j.jseaes.2008.05.011, 2009.

736 Neumann, R. B., Polizzotto, M. L., Badruzzaman, A. B. M., Ali, M. A., Zhang, Z. and Harvey, C. F.: Hydrology
737 of a groundwater-irrigated rice field in Bangladesh: Seasonal and daily mechanisms of infiltration, *Water*
738 *Resour. Res.*, 45(9), 1–14, doi:10.1029/2008WR007542, 2009.

739 Parkhurst, D. L. and Appelo, C. A. J.: Description of Input and Examples for PHREEQC Version 3 — A
740 Computer Program for Speciation, Batch-Reaction, One-Dimensional Transport, and Inverse Geochemical
741 Calculations. U.S. Geological Survey Techniques and Methods, book 6, chapter A43, 497 p., U.S. Geol. Surv.
742 *Tech. Methods*, B. 6, chapter A43, 6–43A, doi:10.1016/0029-6554(94)90020-5, 2013.

743 Paul, B. G. and Vogl, C. R.: Impacts of shrimp farming in Bangladesh: Challenges and alternatives, *Ocean*
744 *Coast. Manag.*, 54(3), 201–211, doi:10.1016/j.ocecoaman.2010.12.001, 2011.

745 Post, V. E. A. and Kooi, H.: Rates of salinization by free convection in high-permeability sediments: insights
746 from numerical modeling and application to the Dutch coastal area, *Hydrogeol. J.*, 11(5), 549–559,
747 doi:10.1007/s10040-003-0271-7, 2003.

748 Rahman, M. M., Hassan, M. Q., Islam, M. S. and Shamsad, S. Z. K. M.: Environmental impact assessment on
749 water quality deterioration caused by the decreased Ganges outflow and saline water intrusion in south-western
750 Bangladesh, *Environ. Geol.*, 40(1–2), 31–40, doi:10.1007/s002540000152, 2000.

751 Ravenscroft, P., Burgess, W. G., Ahmed, K. M., Burren, M. and Perrin, J.: Arsenic in groundwater of the Bengal
752 Basin, Bangladesh: Distribution, field relations, and hydrogeological setting, *Hydrogeol. J.*, 13(5–6), 727–751,
753 doi:10.1007/s10040-003-0314-0, 2005.

754 Santos, I. R., Eyre, B. D. and Huettel, M.: The driving forces of porewater and groundwater flow in permeable
755 coastal sediments: A review, *Estuar. Coast. Shelf Sci.*, 98, 1–15, doi:10.1016/j.ecss.2011.10.024, 2012.

756 Sarkar, A., Sengupta, S., McArthur, J. M., Ravenscroft, P., Bera, M. K., Bhushan, R., Samanta, A. and Agrawal,
757 S.: Evolution of Ganges–Brahmaputra western delta plain: Clues from sedimentology and carbon isotopes, *Quat.*
758 *Sci. Rev.*, 28(25–26), 2564–2581, doi:10.1016/j.quascirev.2009.05.016, 2009.

759 Sengupta, S., McArthur, J. M., Sarkar, A., Leng, M. J., Ravenscroft, P., Howarth, R. J. and Banerjee, D. M.: Do
760 Ponds Cause Arsenic-Pollution of Groundwater in the Bengal Basin? An Answer from West Bengal, *Environ.*
761 *Sci. Technol.*, 42(14), 5156–5164, doi:10.1021/es702988m, 2008.

762 Shameem, M. I. M., Momtaz, S. and Rauscher, R.: Vulnerability of rural livelihoods to multiple stressors: A case
763 study from the southwest coastal region of Bangladesh, *Ocean Coast. Manag.*, 102, 79–87,
764 doi:10.1016/j.ocecoaman.2014.09.002, 2014.

765 Shamsudduha, M. and Uddin, A.: Quaternary shoreline shifting and hydrogeologic influence on the distribution
766 of groundwater arsenic in aquifers of the Bengal Basin, *J. Asian Earth Sci.*, 31(2), 177–194,
767 doi:10.1016/j.jseaes.2007.07.001, 2007.

768 Sharma, B., Amarasinghe, U., Xueliang, C., de Condappa, D., Shah, T., Mukherji, A., Bharati, L., Ambili, G.,
769 Qureshi, A., Pant, D., Xenarios, S., Singh, R. and Smakhtin, V.: The Indus and the Ganges: River basins under
770 extreme pressure, *Water Int.*, 35(5), 493–521, doi:10.1080/02508060.2010.512996, 2010.

771 Sivan, O., Yechieli, Y., Herut, B. and Lazar, B.: Geochemical evolution and timescale of seawater intrusion into
772 the coastal aquifer of Israel, *Geochim. Cosmochim. Acta*, 69(3), 579–592, doi:10.1016/j.gca.2004.07.023, 2005.

773 Smith, A. J. and Turner, J. V.: Density-dependent surface water-groundwater interaction and nutrient discharge
774 in the Swan-Canning Estuary, *Hydrol. Process.*, 15(13), 2595–2616, doi:10.1002/hyp.303, 2001. Steefel, C. I.
775 and Macquarrie, K. T. B.: Approaches to modeling of reactive transport in porous media, *Rev. Mineral.
776 Geochemistry*, 34(1), 85–129, 1996.

777 Stuyfzand, P. J.: A new hydrochemical classification of water types, *IAHS Publ.*, 182, 88–89, 1989. Stuyfzand, P.
778 J.: Hydrochemistry and hydrology of the coastal dune area of the Western Netherlands, Ph.D. thesis, Vrije
779 Universiteit of Amsterdam., 1993.

780 Sukhija, B. S., Varma, V. N., Nagabhushanam, P. and Reddy, D. V.: Differentiation of palaeomarine and
781 modern seawater intruded salinities in coastal groundwaters (of Karaikal and Tanjavur, India) based on inorganic
782 chemistry, organic biomarker fingerprints and radiocarbon dating, *J. Hydrol.*, 174(1–2), 173–201,
783 doi:10.1016/0022-1694(95)02712-2, 1996.

784 Törnqvist, T. E., Wallace, D. J., Storms, J. E. A., Wallinga, J., van Dam, R. L., Blaauw, M., Derksen, M. S.,
785 Klerks, C. J. W., Meijneken, C. and Snijders, E. M. A.: Mississippi Delta subsidence primarily caused by
786 compaction of Holocene strata, *Nat. Geosci.*, 1(3), 173–176, doi:10.1038/ngeo129, 2008.

787 Tóth, J.: A theoretical analysis of groundwater flow in small drainage basins, *J. Geophys. Res.*, 68(16), 4795–
788 4812, doi:10.1029/JZ068i016p04795, 1963.

789 Umitsu, M.: Late quaternary sedimentary environments and landforms in the Ganges Delta, *Sediment. Geol.*,
790 83(3–4), 177–186, doi:10.1016/0037-0738(93)90011-S, 1993.

791 van der Sluijs, P., Steur, G. G. L. and Ova, I.: DE BODEM VAN ZEELAND, toelichting bij blad 7
792 van de Bodemkaart van Nederland, schaal 1 : 200 000, 1965

793 van Gaans, P. F. M., Griffioen, J., Mol, G. and Klaver, G.: Geochemical reactivity of subsurface sediments as
794 potential buffer to anthropogenic inputs: a strategy for regional characterization in the Netherlands, *J. Soils
795 Sediments*, 11(2), 336–351, doi:10.1007/s11368-010-0313-4, 2011.

796 Van Santen, P., Augustinus, P. G. E. F., Janssen-Stelder, B. M., Quartel, S. and Tri, N. H.: Sedimentation in an
797 estuarine mangrove system, *J. Asian Earth Sci.*, 29(4), 566–575, doi:10.1016/j.jseaes.2006.05.011, 2007.

798 Vlam A. W.: Historisch-morfologisch onderzoek van eenige Zeeuwsche eilanden, Ph.D thesis, Utrecht
799 Universiteit., 1942.

800 Walraevens, K., Cardenal-Escarcena, J. and Van Camp, M.: Reaction transport modelling of a freshening aquifer
801 (Tertiary Ledo-Paniselian Aquifer, Flanders-Belgium), *Appl. Geochemistry*, 22(2), 289–305,
802 doi:10.1016/j.apgeochem.2006.09.006, 2007.

803 Worland, S. C., Hornberger, G. M. and Goodbred, S. L.: Source, transport, and evolution of saline groundwater
804 in a shallow Holocene aquifer on the tidal delta plain of southwest Bangladesh, *Water Resour. Res.*, 51(7), 5791–
805 5805, doi:10.1002/2014WR016262, 2015.